Journal of CO2 Utilization 105 (2026) 103351

Contents lists available at ScienceDirect

Journal of CO2 Utilization

journal homepage: www.elsevier.com/locate/jcou

# Carbon dioxide capture from air in buildings – Design and techno-economic feasibility of practical systems

Dominik Heß *, Michael Rubin, Roland Dittmeyer

*Institute for Micro Process Engineering (IMVT) at Karlsruhe Institute for Technology (KIT), Hermann-von-Helmholtz-Platz 1, Eggenstein-Leopoldshafen 76344, Germany*

ARTICLE INFO

*Keywords:*
Direct Air Capture (DAC)
Carbon Dioxide Capture
Temperature Vacuum Swing Adsorption (TVSA)
Heating, Ventilation and Air Conditioning (HVAC)
Negative Emissions Technology (NET)
Levelized Costs of Direct Air Capture (LCOD)

ABSTRACT

Direct Air Capture (DAC) is needed alongside other $CO_2$ removal methods to ensure that the total amount of $CO_2$ required is removed from the atmosphere so that global warming can be limited to below 2 °. While large-scale DAC farms are a promising solution, their high CAPEX and OPEX, along with societal concerns, may hinder widespread deployment. This study presents a novel, modular DAC concept designed for integration into heating, ventilation, and air conditioning (HVAC) systems of buildings. A prototype was engineered and modeled in MATLAB to analyze key physical processes in the adsorber bed using two amine-based adsorbents. A linear driving force model was applied to simulate mass transport, and the DAC unit was coupled with an HVAC system in Simulink to evaluate $CO_2$ capture from indoor air. Solar thermal energy with thermal storage was defined as the heat source. Optimization results indicate a 40 % reduction in thermal energy demand compared to separate DAC and HVAC systems. Cold, humid air improves $CO_2$ capture, while dry air significantly lowers the energy demand – up to 50 % when reducing humidity from 90 % to 10 %. A techno-economic analysis suggests that mass-produced DAC modules for HVAC systems could achieve levelized costs of DAC as low as 280 € per ton $CO_2$, particularly when waste heat is utilized. Implementation in densely occupied buildings may yield additional savings of up to 9 %. This work highlights the potential of HVAC-integrated DAC systems as a scalable, cost-effective complement to centralized DAC facilities.

## 1. Introduction

In 2015, at the UN Climate Change Conference (COP21), 196 countries agreed to take action against the anthropological climate change (Paris Agreement, [1]). The core action defined is the massive reduction in greenhouse gas (GHG) emissions and ultimately the avoidance of them altogether, in order to limit global warming well below 2°C above pre-industrial level in the long term. For example, the remaining carbon budget for a 50 % likelihood to limit global warming to 1.5, 1.7, and 2 °C above the 1850–1900 level has been reduced to 65 $Gt_C$ (235 $Gt_{CO2}$), 160 $Gt_C$ (585 $Gt_{CO2}$), and 305 $Gt_C$ (1110 $Gt_{CO2}$), respectively, from the beginning of 2025, equivalent to around 6, 14, and 27 years, assuming 2024 emissions levels [2]. Removal and storage (Carbon Capture and Storage, CCS) of $CO_2$ from the atmosphere or point sources can act in two ways: Net negative emissions to prevent or reverse a possible overshoot of the emissions or allowing for net zero emissions by capturing $CO_2$ emissions of emitters that are hard to decarbonize resp. to compensate such emissions. Among those are emissions caused by the aviation and transport sector (especially heavy load transportation, shipping, aviation) or industrial processes such as of the cement industry. Besides, in a post-fossil economy, $CO_2$ will become a valuable feedstock for the chemical industry, since it can serve as carbon source for synthetic hydrocarbons, polymers, etc. (Carbon Capture and Utilization, CCU). Thus, it is of crucial importance to capture $CO_2$ not only from high concentrated point sources but also from thin air [3,4].

One option is biogenic $CO_2$ capture using plants and algae to capture atmospheric $CO_2$ and fix it in biomass. When using that biomass by incineration or fermentation, the $CO_2$ is released again, but in a concentrated form and can be captured from such point sources for e.g. storage, also known as BECCS concept (Bioenergy with CCS) [5–7]. Another option is to capture the $CO_2$ directly from the air using a so-called Direct Air Capture (DAC) technology [8].

Generally speaking, DAC summarizes all technological solutions to separate $CO_2$ from the air. Basic principle is that for the capturing step a special material is used which reacts/interacts selectively with $CO_2$ and barely with other components of the air [9].

In the last years two types of DAC technologies have developed towards higher technology readiness levels, namely high- and low-

* Corresponding author.
*E-mail address:* dominik.hess2@kit.edu (D. Heß).

https://doi.org/10.1016/j.jcou.2026.103351
Received 21 December 2025; Received in revised form 26 January 2026; Accepted 2 February 2026
Available online 13 February 2026

temperature-DAC (HT-, resp. LT-DAC) [8,10]. Since this study focuses on DAC units integrated in HVAC systems in the near future, other DAC options of lower technology readiness level (TRL) even though promising (e.g. electro swing adsorption [11,12]) are not considered here.

HT-DAC is based on a liquid sorbent such as potassium hydroxide solutions forming potassium carbonate in the capturing step which needs to be regenerated to the accordant base via a multi-step process, partially at high temperatures (up to 900°C) [13]. High temperature processes are inherently prone to large scales to make them efficient, which is why the leading company in that field, carbon engineering, is aiming to roll out the technology in one megaton per year plants [14]. Those scales are not feasible in a building environment and therefore HT-DAC is ruled out as viably option for decentralized DAC systems considered in this study.

LT-DAC on the other hand can be scaled rather freely. It is based on chemisorption of $CO_2$ on a solid sorbent material usually functionalized by amine groups [15–17]. There are some studies using other sorbents such as metal organic frameworks (MOFs), but so far no commercial application is in sight [18,19]. The geometry and shape of the adsorber and the active sorbent material may vary (e.g. packed bed vs. monoliths), but obviously in every LT-DAC system air needs to be contacted with the solid sorbent to capture the $CO_2$. After saturating the sorbent material, regeneration is usually done by increasing temperature and decreasing pressure. LT-DAC therefore is a Temperature-Vacuum-Swing-Adsorption (TVSA) process. In the regeneration step, before thermal energy is introduced, the remaining air is evacuated from the adsorber unit to avoid contamination of the $CO_2$, to promote desorption, and to protect the sorbent material from degradation by oxidation. Then, the system is heated up to usually around 100°C ('low temperature'). In practice, heat is either supplied by simply using heating coils, or, more widely used, by steam injection, which not only introduces heat by its high heat capacity but also by its condensation enthalpy. In addition, steam further acts as a carrier stream for the released $CO_2$ which, after condensing the steam, is obtained in high purity.

LT-DAC plants are by nature modular and, thus, easily scalable. With a nameplate annual capacity of 36,000 tons of $CO_2$, and being currently in commissioning and ramp-up phase, Climework's Mammoth demonstration plant will be the largest LT-DAC plant [20]. Other companies aim also for small, decentralized applications like soletair (LT-DAC in buildings [21]) or Skytree (LT-DAC for controlled environment agriculture [22]).

As LT-DAC allows for simple scaling due to its modular nature, it does not require toxic/harmful chemicals in the process, and further can be easily automated and, thus, run safely in remote operation, LT-DAC is the DAC concept of choice when discussing the implement into HVAC system. Therefore, LT-DAC is set as the basis for this study, in which focus is laid on the investigation of implementing LT-DAC into ventilation systems concerning quantification of energy-related synergies and how such a coupled system needs to be operated in order to eventually reduce CAPEX and OPEX as compared to standalone DAC.

There has been research investigating coupled HVAC/DAC systems, but mainly with a focus on air quality [23–25], rather than utilizing synergies for lowering the levelized cost of DAC (LCOD). However, quite recently there has been a comprehensive study by Xu et al. investigating the energy savings potential of DAC integrated into the HVAC systems, coming to the conclusion, that up to ~22 % annual energy savings with additional carbon emissions reduction is feasible, proving the merit of this approach [26].

The combination of such a HVAC/DAC- system with a direct conversion of the captured $CO_2$ into hydrocarbon fuels in decentralized plants which could then be viewed as distributed "renewable oil wells" was proposed by Dittmeyer et al. under the name "Crowd Oil" in a perspective article back in 2019 [27]. This paper connects to that vision and provides technical details and cost estimates for the captured $CO_2$. As the initial $CO_2$ concentration affects the rate of $CO_2$ capture (via sorption kinetics), using air from buildings (usually ≥700 ppm $CO_2$ and more [28]) as a feed stream for DAC can increase energy efficiency resp. decrease cycle time/built size as compared to systems using outside air (~400 ppm $CO_2$ [29]). The minimal thermodynamical separation work, i.e. the lowest possible energy demand lies at 138 kWh $t_{CO2}^{-1}$ for 400 ppm and 129 kWh $t_{CO2}^{-1}$ for 700 ppm [30], showing a substantial potential for energy efficiency gains, if compared to current estimates for DAC energy consumption in the range of 1300–2500 kWh $t_{CO2}^{-1}$ [13,30–33].

Therefore, the goal of this work lies in the thorough investigation of the behavior of an integrated HVAC/DAC-system, identifying energy synergies, optimal operating strategies, and the capture capacity. That insight will then help analyzing the most important economics of the system by calculating the LCOD, identifying the most cost-effective versions, while also ensuring the safe and undisturbed operation of the ventilation system.

For that matter the DAC unit itself has been modelled mathematically as a fixed bed adsorber with the regeneration being done using direct steam injection. Further, the whole system consisting of the DAC-adsorber, the ventilation system, the building, modules for solar thermal heat generation and a thermal energy storage has been simulated. Using dynamic input variables, the behavior of a real-world application has been approximated, including diurnal variations of solar power, building occupancy and temperature. Finally, a techno-economic analysis of such a system is done to evaluate the feasibility of its application.

## 2. Methods

### 2.1. General description of the HVAC/DAC system and assumptions made

The system considered consists of components that are already present in a standard system of a building equipped with a ventilation system, namely the building itself, a fan, and a control system, as well as additional components, namely renewable energy supply via solar thermal heat, a heat storage, and the DAC-unit (as mentioned, in the following only LT-DAC is considered). Each component is interconnected as shown in Fig. 1.

Simulink is used to implement the flowsheet simulation and to calculate the respective mass and energy streams. The DAC-module is considered via an embedded Matlab model, which is described in Section 2.2 in detail. All simulations have been run for 72 h simulated time, where the first 24 h have been disregarded in the evaluation to ensure a properly run-in time. Since the physical processes during adsorption are comparably slow, time steps of 120 s were defined in the simulation, while the desorption step is simulated with 5 s intervals. There are in general two options to connect the DAC unit into the system. The first is to set it upstream the building (light grey arrows in Fig. 1). In that way ambient air is fed to the DAC, which is subject to diurnal temperature variations and different humidity levels. The intake air then always has a rather constant $CO_2$ concentration (400 ppm) and the further $CO_2$

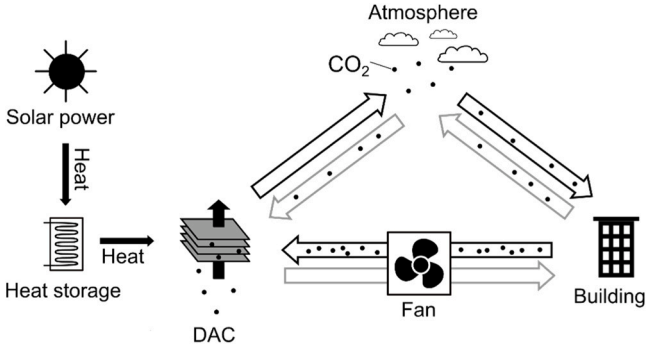


**Fig. 1.** Schematic of the considered building integrated DAC coupled with the ventilation system.

depleted air is fed into the building. In this configuration, potential deactivating substances, that might be within the buildings (e.g. industrial hall, chemical laboratories, etc.) exhaust stream, are not injected into the DAC. Additionally, the $CO_2$ level in the building is kept below ambient conditions, possibly benefiting the occupants' mental abilities. The second option is the implementation of the DAC-unit downstream the building (black arrows in Fig. 1). In this configuration the DAC benefits from an increased $CO_2$ concentration due to e.g. respiration of the building's occupants. The temperature and humidity then remain at a rather constant level, set by the building air conditioning (AC) system while $CO_2$ concentration potentially varies over the course of a (working) day.

The DAC unit itself consists of the adsorber module containing the sorbent material as well as a steam cycle, that delivers superheated steam for regeneration. Details are explained in Section 2.2.9. As ventilation systems substantially vary in size, it is reasonable to use a modular design, i.e. small standardized units, that can operate individually or in a larger consolidation. This would allow to use just a portion of the ventilation capacity for the DAC retrofitting and/or to gradually implement an ever-larger DAC-capacity.

The approach followed in this study is therefore to define a standardized HVAC/DAC-unit, further described and discussed in Section 2.2, combining the relevant infrastructure of the ventilation with an accordantly sized DAC-module, designed to fit most commercially used buildings. Boundary conditions, such as physical dimensions or expected air flow rates are exemplarily taken from the existing ventilation system of the authors' affiliating Institute (Institute for Micro Process Engineering (IMVT) at the Karlsruhe Institute of Technology (KIT, Karlsruhe, Germany), "reference building" in the following), as all relevant information were accessible for this study without constraints and further, two commercial DAC modules, each with a capacity for capturing about 100 kg of $CO_2$ per day are currently being installed in the HVAC system to provide an experimental demonstrator:

- Pressure drop: To limit the additional installation of ventilation power to cheap axial fans or to enable the existing infrastructure to handle the additional load, a maximal pressure drop of 150 Pa has been set at nominal airflow. This would lead to a theoretical minimal energy demand of 115 kWh $t_{CO2}^{-1}$ for moving the air which is in accordance or lower to numbers from the DAC companies [13,31].
- Adsorber bed dimensions: Because building infrastructure is usually installed in confined spaces, the physical dimensions have to be kept manageable. The institutes system is used as a reference and would allow for two cylindrical packed beds with max. 3 m diameter (or other shaped with similar area), while the length will be determined by the pressure drop. This is an assumption based on the reference building, as here the fresh air is provided by two separate ducts to two equally sized parts of the building. Each duct is 1 m in diameter and installed freely on the rooftop with no vertical obstruction and enough free space left and right to accommodate the adsorber beds.
- Unit size: For the option of mass manufacturing numerous DAC units, a standard module fitting the reference HVAC system with its 22,000 $m^3h^{-1}$ air flow rate, split into two stands fed with equal flow rate (11,000 $m^3h^{-1}$) and both equipped with one adsorber bed was defined. Higher capacities would mean further parallelization.
- Capture Efficiency: Over the course of one ad-/desorption cycle a minimal average capture efficiency $\eta_{Cap} = 50$ % must be achieved.

Further, in analogy to Ref. [27], the general potential of such a system was assessed on the basis of (a) the landmark building "Messeturm" in Frankfurt am Main (Germany) denoted as prototypical "Office Building" (OB) with a floor area of approx. 60,000 $m^2$ with 4000 workplaces and an assumed inside air volume and ventilation capacity of approx. 180,000 $m^3$ and 1000,000 $m^3$ $h^{-1}$, respectively. Besides, in order to evaluate the effect of $CO_2$ enrichment by the occupants of such a building, two additional use cases were considered: (b) use case of an open-plan office, OPO (up to 10,000 occupants representing the maximum allowed density of workplaces in an office according to the workplace guidelines ("Arbeitsstättengesetz") in Germany, where the building is situated [34]), and (c) the use case of a warehouse, WH. In all three scenarios (OB, OPO, WH), inside temperature and humidity can be assumed to be constant. However, in the use-case scenario OPO $CO_2$ levels are higher than in the OB scenario and in the WH scenario no or only a negligible number of workers are present, thus, $CO_2$ concentration is rather constant at atmospheric level. In the latter case (WH) the DAC unit is fed by air at constant temperature and humidity levels like in the cases of OB and OPO, but in the WH-scenario the $CO_2$ level does not increase inside the building, and therefore serves as a base case scenario in terms of capacity and energy demand in this study.

The results presented in the following are always given for these prototype buildings for which 45 of the above-mentioned standard units (22,000 $m^3h^{-1}$ air flow rate each) are assumed to be installed in parallel.

To increase the significance of the results, two different adsorbent materials are considered with characteristic data taken from literature. The primary material is a amine-functionalized nano-cellulose (NC) from Climeworks, with data originating from a study by the company [16], [35] and Lewatit VP OC 1065 (LW) with data from the manufacturer Lanxess and a study by Young et al. [36,37]. The specifics of the adsorption process are explained in chapter 2.2 in detail.

The general cyclic operation follows a TVSA scheme and, thus, can be divided into two major steps, (1) $CO_2$-capture via adsorption and (2) sorbent regeneration (i.e. $CO_2$ release), wherein the regeneration itself consists of the three consecutive steps (2a) evacuation, (2b) steam injection and (2c) cooling:

In the capture step (1), air is moved through the packed bed at the specified volumetric flow rate. The $CO_2$ binds covalently to the functionalized groups at the sorbent's surface and the $CO_2$ depleted air leaves the unit. When the adsorber is sufficiently saturated with $CO_2$, the capture step is terminated. Since there is no straight forward way to directly measure the $CO_2$ content on the sorbent material itself, the $CO_2$ concentration of the entering resp. leaving air is taken as an indirect measure. Either a maximum outlet concentration $c_{CO2,out}$ is defined or the capture efficiency $\eta_{Cap}$ is determined as criterion:

$$\eta_{Cap} = 1 - \frac{c_{CO2,out}}{c_{CO2,in}} \quad (1)$$

The first part of the regeneration is the evacuation (2a). The vacuum pump removes air from the sorption chamber until a total pressure of 0.1 bar is reached to limit the contamination of the $CO_2$ by oxygen and nitrogen and to prevent oxidation i.e. deactivation of the adsorber material. Subsequently, steam at 100°C (superheated at the present pressure level) is injected into the packed bed (2b) causing the desorption of $CO_2$ which leaves the DAC unit together with the flow of water vapor until the adsorber is sufficiently unloaded. For the following cooling step (2c), steam at 45°C/0.1 bar is injected to reduce the adsorber's temperature to at least 60°C in order to avoid oxidation and therefore degradation of the material. After cooling, one cycle is completed and capture (1) is started over again.

### 2.2. Implementation of sub-models for modelling DAC/HVAC on a systems level

#### 2.2.1. Building

The building and its ventilation system are central to the simulation with the most important task being to keep the $CO_2$ concentration of the indoor air low enough to be healthy for human beings. The German Environment Agency (UBA, equivalent to EPA in the US) defines the air quality according to certain $CO_2$ concentration ranges [38]: High (< 800 ppm), medium (800 – 1000 ppm), moderate (1000 – 1400 ppm) and low (> 1400 ppm) air quality.

In this study, the current $CO_2$ concentration in the building is modelled by applying the continuously stirred tank reactor (CSTR)

concept for the building's volume $V_{Buil}$, where air enters at ambient conditions ($\dot{V}_{air}$, $c_{CO_2,in}$), and leaves the building at the current building $CO_2$ concentration ($c_{CO_2,out}$) being higher due to the $CO_2$-generation $\dot{G}$ by the respirating people within the building. Complete back mixing and no leakages were assumed. The material balance for $CO_2$ is:

$$V_{Buil}\frac{dc_{CO2}}{dt} = \dot{V}_{air}\left(c_{CO2,in} - c_{CO2,out}\right) + \dot{G}(t) \quad (2)$$

The total $CO_2$-generation rate $\dot{G} = \dot{g} \bullet n_{people}$ is given by the respirating of the $n_{people}$ people within the building, with a per person $CO_2$ generation rate $\dot{g}$ of 4.8 $ml_{CO2}$ $s^{-1}$ $Person^{-1}$ according to a study by Persily [39] considering all people doing office work.

The $CO_2$ generation rate is directly linked to the number of people $n_{people}$ present in the building. Typically, the occupancy varies over the day, which is why in the simulation the occupancy is approximated by a smooth square function (equation S1), being zero at night from 6 pm to 6 am and ramps up smoothly to the maximal count of people $n_{people,max}$ (WH: 0, OB: 4000, OPO: 10,000).

By integrating the differential Eq. (2) with the current ($c_{CO2,0}$) and new ($c_{CO2}$(t)) $CO_2$-concentration as boundaries, and assuming the exit concentration equals the one within the volume (ideal CSTR assumption), the following Eq. (3) describes the $CO_2$-level after a certain time $t$ with constant input parameters.

$$c_{CO2}(t) = c_{CO2,in} - \frac{\left[\dot{V}_{air}\left(c_{CO2,in} - c_{CO2,0}\right) + \dot{G}\right]\cdot e^{\frac{\dot{V}_{air}}{V_{Buil}}\bullet t} - G(t)}{\dot{V}_{air}} \quad (3)$$

If $\dot{V}_{air}$ is zero, the solution for the ODE in Eq. (3) simplifies to:

$$c_{CO2}(t) = c_{CO2,0} + \frac{\dot{G}(t)}{V_{Buil}} \bullet t \quad (4)$$

### 2.2.2. Fan operation strategy and pressure drop

The fan draws air from the outside and pushes it through the building including the adsorber (upstream or downstream the building). The volumetric flow rate $\dot{V}_{air}$ is either controlled by a PID controller or set at the nominal flow rate. For the controlled operation, the input is the difference in $CO_2$-concentration of the building to a predefined set point (SP). The PID-Parameters are listed in Table S1. The chosen setpoints in this work are defined at 700 ppm and 1000 ppm corresponding to high air quality and transition from medium to moderate air quality, respectively, according to the definition by the German Environment Agency (UBA) [38] as mentioned above.

The additional power $P_{Fan,add}$ required to push air through the DAC unit is calculated with the respective pressure drop $\Delta p$ of the DAC unit (s). Details are given in the Supplementary Material (S1.3).

### 2.2.3. Solar thermal heat

In the envisioned concept, solar thermal energy is considered to provide renewable heat for the regeneration of the adsorbent. Like the dimensions of the DAC-unit, the peak power of the solar thermal plant has been chosen to be a realistic fit for the reference building. (35 kWp). With 0.7 kW peak per square meter in central europe as realistic number for a modern solar thermal plant, 50 square meters of roof area would have to be covered, well within the dimensions of the reference building [40]. To simulate the temporal power fluctuations, a generic diurnal function has been set up, by fitting a polynomial of grade six to a solar irradiation curve from Ile-Ife, a city near the equator [41], representing a sunny day with good conditions for renewable power generation. This curve has then been normalized (see Fig. S1) and multiplied with the above-mentioned peak power to get the currently available power information.

### 2.2.4. Outside air temperature and humidity

When the DAC is integrated upstream the building, outside air temperature affects $CO_2$ adsorption during the capture process. The current outside temperature is determined similar to the solar power, described in Section 2.2.3, by fitting a polynomial of grade six to the diurnal variation of the air temperature. Unlike the solar power, the temperature curve is not normalized, but y-shifted so that the lowest value is set at a defined base temperature $T_{Base}$. Depending on the specific climatic case, $T_{Base}$ is adjusted. The humidity is assumed to be constant throughout the day. One example would be a hot and dry desert climate with only 10 % relative humidity and a diurnal temperature variation from $T_{Base}$= 25°C to 33°C.

### 2.2.5. Heat storage

As renewable power fluctuates throughout the day (compare Section 2.2.3), a heat storage is implemented conceptually to allow for continuous operation of the DAC unit. The heat storage is simulated using an integrator block adding the incoming power from the solar thermal plant and subtracting the heat flux used by the DAC unit. The heat storage has a capacity limit which can be adjusted. In this study, the size of the heat storage was adjusted to 120 kWh, in order to allow for continuous operation.

### 2.2.6. Vacuum pump

As outlined above, a vacuum pump is needed to remove the air from the sorption chamber prior to its regeneration in order to avoid contamination of the $CO_2$ and oxidation of the sorbent. Additionally, the pump must hold the desorption pressure during regenerating by conveying wet $CO_2$ off the condenser. The power $P_{Vac}$ required was calculated using the first law of thermodynamics and the isentropic expansion equation [42], see Supplementary Information for details.

### 2.2.7. Sorbent material and physico-chemical properties

Aiming for an understanding of the whole HVAC/DAC process, it is crucial to model the mass transport processes within the bed. In this study the mathematical models are implemented in Matlab R2023 based on the following physico-chemical characteristics. All isotherm data are derived from literature, as experimental evaluations of adsorbent materials was not in the scope of this work.

Since the exact material used in commercial DAC-units is not disclosed, sorption data is taken from Wurzbacher and Gebald et al. [16, 35], for an amino-functionalized nanocellulose (NC) sorbent. Due to its high porosity and therefore high surface area, it offers a low pressure drop. Both publications are linked to the company Climeworks, since Wurzbacher and Gebald are two of the founders and the company is mentioned in the Acknowledgments as project partner [16,35]. In their work, the authors found, that the presence of water in the air enhances the uptake of $CO_2$. Therefore, both components must be considered, when modelling the DAC unit. The pure component isotherm for water follows a Guggenheim-Anderson-de Boer (GAB) model [17,35]:

$$q_{H_2O} = C_m(T)\frac{C_G K_{ads}(T)\varphi}{(1 - K_{ads}(T)\varphi)(1 + (C_G - 1)K_{ads}(T)\varphi} \quad (5)$$

With $\varphi$ being the relative humidity, $C_m$ the water capacity of a single layer, $K_{ads}$ and $C_G$ temperature depending coefficients describing multilayer adsorption and $q_{H_2O}$ the water loading of the adsorbens in $mol_{H2O}$ $kg_{Ads}^{-1}$.

The single component isotherm for $CO_2$ on the other hand is described using a Toth isotherm, an expanded Langmuir model [17,35, 43] :

$$q_{CO2} = n_S(T)\frac{b \cdot p_{CO2}}{(1 + (b \cdot p_{CO2})\tau)^{1/\tau}} \quad (6)$$

with $n_S$ being the maximum $CO_2$ loading and b an $CO_2$-affinity parameter.

In Ref. [35] Wurzbacher and Gebald et al. fitted the multicomponent adsorption by first calculating an enhancement factor (Eq. (7)) in order

to include the promoting effect of water on the overall $CO_2$-loading (Eq. (8)). The increase can be quite significant: At a $CO_2$ partial pressure of 40 Pa in air (i.e. 400 ppm at ambient pressure) the $CO_2$ capacity of the adsorbent material can be increased by about 60 %, when increasing the relative humidity $\varphi$ from 0 % to 100 %.

$$f_{RF} = 1 + \varphi\left(0.6 - \frac{p_{CO2}}{5900Pa}0.47\right) \tag{7}$$

$$q_{CO2,wet} = q_{CO2} \cdot f_{RF} \tag{8}$$

Apart from slightly different adsorption isotherms to what was described above, the alternative sorbent material considered in this study, Lewatit, requires a different adsorber bed design, because the small and dense particles result in a very different flow characteristic. This alternative design is further described in Section 3.2.4. Young et al. [17,36] investigated the isotherms and fitted the sorption isotherms likewise using a GAB and Toth model for water and $CO_2$ adsorption, respectively. However, the authors did consider the promotion effect by water not via an enhancement factor but by determining a weighted average dual site Toth co-adsorption model (WADST) based on both, a dry and a wet Toth isotherm for $CO_2$. The WADST is calculated using the following equation:

$$q_{CO2,wet} = \left(1 - e^{-\frac{A}{q_{H2O}}}\right) \frac{q_{\infty,dry} b_{dry} p_{CO2}}{\left(1 + \left(b_{dry} p_{CO2}\right)^{\tau_{dry}}\right)^{\frac{1}{\tau_{dry}}}} + \left(e^{-\frac{A}{q_{H2O}}}\right) \frac{q_{\infty,wet} b_{wet} p_{CO2}}{\left(1 + \left(b_{wet} p_{CO2}\right)^{\tau_{wet}}\right)^{\frac{1}{\tau_{wet}}}} \tag{9}$$

The detailed physico-chemical properties of the two sorbent materials considered, namely nanocellulose and Lewatit VP OC 1065 are listed in SI, Table S2 and S3.

### 2.2.8. Modelling of the adsorber unit

The DAC-sorption chamber is modeled using a 1D flow model with axial dispersion with the following assumptions and specifications:

- Quasi one dimensional system
- Axial dispersion to account for radial flow velocity profiles and back-diffusion in axial direction
- Ideal gas law is applicable
- Only $CO_2$ and water vapor adsorb
- Fluid and solid phase are in thermal equilibrium
- Adiabatic behavior
- Isobaric fluid phase
- No change in volume flow due to adsorption or desorption (share of adsorptives negligible)
- No condensation, but multilayer adsorption of water
- Spherical particles of equivalent diameter of 5.6 mm (NC) resp. 0.52 mm (LW) (see Section 2.2.2 and SI)

The main differential equations, solved via a finite differences method (FDM), are the material balances for the two adsorbing components $i$ ($i$: $CO_2$, water). A dispersion model has been utilized to account for the effects of radial flow velocity profiles and back-diffusion in axial direction [44]:

$$\frac{\partial c_i}{\partial t} = D_{ax,i}\frac{\partial^2 c_i}{\partial z^2} - u\frac{\partial c_i}{\partial z} - \rho_S \frac{1 - \epsilon_{tot}}{\epsilon_{tot}}\frac{\partial q_i}{\partial t} \tag{10}$$

$D_{ax,i}$ is the axial dispersion coefficient, $u$ the interstitial gas velocity, $\rho_S$ the solid density and $\epsilon_{tot}$ the total porosity of the bed (incl. intra-particle porosity $\epsilon_{Part}$).

The axial dispersion coefficient is calculated using a correlation by Edwards [45]:

$$\frac{D_{ax,i}}{d_{Part}u} = \frac{1}{Pe} = \frac{0.73\epsilon_{bed}}{ReSc} + \left(2\left(1 + \frac{0.7313\epsilon_{bed}}{ReSc}\right)\right)^{-1} \tag{11}$$

The kinetics of adsorption are calculated using a linear driving force (LDF) model:

$$\frac{\partial q_i}{\partial t} = k_{LDF,i} \cdot \left(q_i^*(T) - q_i\right) \tag{12}$$

The LDF parameter $k_{LDF,i}$ is determined using the mass transport resistances in the film and volume while $q_{i,0}^*(T)$ is the equilibrium loading given by the adsorption isotherms of the corresponding materials, here Eqs. (5) and (6) [44], [46]:

$$k_{LDF,i} = \left(\frac{d_{Part} q_{i,0}^* \rho_S (1 - \epsilon_{Part})}{6\beta_i c_{i,0}} + \frac{d_{Part}^2 q_{i,0}^* (1 - \epsilon_{Part})\rho_S}{60 c_{i,0} D_{eff,i} \epsilon_{Part}}\right)^{-1} \tag{13}$$

The mass transfer coefficient $\beta_i$ is obtained by a Sherwood correlation:

$$Sh_i = \frac{\beta_i d_{Part}}{D_{m,i}} \tag{14}$$

Here, $D_{m,i}$ is the molecular diffusion coefficient. $D_{eff,i}$ can be approximated via Eq. (15), while the pore diffusivity $D_{Pore}$ is a combination of Knudsen and molecular diffusion [47] (Eq. (16)).

$$D_{eff,i} = D_{Pore}\epsilon_{Part}\frac{1}{\tau} \tag{15}$$

$$\frac{1}{D_{Pore}} = \frac{1}{D_{Knudsen}} + \frac{1}{D_m} \tag{16}$$

For the molecular diffusion coefficient, the correlation by Fuller-Schettler-Giddings has been used [48]:

$$D_{m,i} = D_{A,B} = T^{1.75}\left(\frac{1}{M_A} + \frac{1}{M_B}\right)^{0.5} \cdot p\left(\nu_A^{\frac{1}{3}} + \nu_B^{\frac{1}{3}}\right)^{-2} \tag{17}$$

After closing the material balances and determining the current concentration of $CO_2$ and water in the bulk gas phase and consequently the adsorbent loading in all cells, the energy balance and thereby the temperature profile in the unit can be determined via Eq. (18) [44]. Here, the enthalpy of the fluid phase as well as conduction, convection, and the heat of adsorption are taken in account. Since the unit is considered adiabatic, the influence of the wall temperature can be neglected.

$$\left(\epsilon_{Tot}\rho_f c_{p,f} + \left(1 - \epsilon_{Tot}\rho_S c_{p,S}\right)\right)\frac{\partial T}{\partial t} = -u\epsilon_{tot}\rho_f c_{p,f}\frac{\partial T}{\partial z} + k_{eff,i}\frac{\partial^2 T}{\partial z} + (1 - \epsilon_{tot}\rho_S)\sum_i\left(\frac{dq_i}{dt} \cdot - \Delta h_{ads,i}\right) \tag{18}$$

### 2.2.9. Steam cycle and heat demand

In order to evaluate the optimal process configuration for providing the thermal energy for regeneration of the DAC unit, three concepts have been assessed in this study: an idealized steam cycle and two more realistic alternatives considering real heat transfer characteristics. All three considered configurations rely on a steam cycle including a superheater (powered by electricity or an external heat source) right before the DAC unit to superheat the steam to 100°C at 0.1 bar(a). The overheated steam further drives the desorption in the adsorber bed. Unless otherwise stated, for the heaters implemented in the three different steam cycles, maximum efficiency for the energy balance is assumed (i.e. $P_{th,required} = P_{el,provided}$).

- Idealized steam cycle (see SI Fig. S2) – in this idealized configuration, after leaving the sorption chamber, the steam is cooled down to

10°C, i.e. condensed, in a heat exchanger providing the energy for feed water evaporation. The desorbed $CO_2$ is eventually retained in a downstream gravimetric separator via a vacuum pump. Water loss (due to the remaining water in the $CO_2$/water mixture at 10°C/0.1 bar(a)) is replenished at likewise 10°C/0.1 bar(a). This idealized cycle therefore assumes ideal heat transfer with zero losses, i.e. full heat recovery, and therefore can show the behavior of the adsorber bed without interference of the steam cycle.

- Steam cycle with heat pump integration (see SI Fig. S3) – Here, the cooling is split into two steps: First the $CO_2$/steam mixture leaving the sorption chamber is cooled in a heat exchanger against saturated steam before condensation. The heat of condensation is used to evaporate the feedwater. Since there must be a driving temperature gradient, the heat is driven through a heat pump from condensation to steam generation. The water/$CO_2$ mixture is still at 45°C, when it enters the first separator. The remaining steam is then further cooled down to 10°C and the additional condensate is withdrawn in a second separator before the still gaseous water/$CO_2$ mixture (10°C/0.1 bar(a)) leaves the system via a vacuum pump. Water loss is replenished at likewise 10°C/0.1 bar(a) and fed to the evaporator/condenser combination for its evaporation via the heat pump. The heat pump is assumed to have a high coefficient of performance (COP) of 5.
- Steam cycle with different pressure levels (see SI Fig. S4) – Here, the necessary temperature gradient in the condenser/evaporator unit is achieved by implementing an exhaust vapor compressor, which increases the pressure of the steam/$CO_2$ mixture leaving the sorption chamber to 0.15 bar(a) and therefore the dew point up to 55°C. Thereby a temperature difference between the condensation (55°C/0.15 bar(a)) and fresh water evaporation (45°C/0.1 bar(a)) of 10 K is given. Gas-liquid separation is likewise implemented as in two steps, here operated at 55°C/0.15 bar(a) and 10°C/0.1 bar(a), respectively. The feed water on the other side is partially evaporated by decreasing the pressure below vapor pressure (55°C/0.15 bar(a) to 55°C/0.1 bar(a)) and further in the condensation-evaporation unit before being superheated by the superheater. The additional power required for the compressor is calculated in analogy to Eq. (S4).

### 2.3. Techno-economic analysis

The results of the simulation study have been used for a techno-economic analysis (TEA) in order to assess the economic feasibility of integrating DAC units into HVAC systems. The levelized cost of DAC (LCOD) being an important metric for DAC systems has been calculated according to Fasihi et al. [33] who adapted a method to calculate the levelized cost for water (LCOW) of desalination plants as of today [49] and projected into the future [50] for calculating $CO_2$ prices, Eq. (19) [49,50]. Energy consumption data and plant capacity/output was derived from the simulations described above in detail. Acquired offers for the main components of the system depicted in SI Fig. S2 – S4, multiplied with a Lang-factor of 3.9, being a typical value for low TRL chemical plants, served as a basis for estimating the capital expenditures (capex) [51]. The fixed operational expenditures $opex_{fix}$ are obtained as a percentage of 3.7 % of the capex, an assumption taken from Fasihi et al. [33]. In the following, only the energy costs are allocated to the variable $opex_{var}$.

$$LCOD = \frac{capex \cdot crf + opex_{fix}}{Output_{CO2}} + opex_{var} \tag{19}$$

Where *crf* is the capital recovery factor, which can be calculated using a weighted average cost of capital (WACCS) of 7 % and the lifetime N (here: 20 years) [33]:

$$crf = \frac{WACC \cdot (1 + WACC)^N}{(1 + WACC)^N - 1} \tag{20}$$

The LCOD obtained by this method is applicable to the prototype plant. To assess future cost, a capex reduction due to future developments and cost saving effects by e.g. mass fabrication is assumed. For this, a log-linear learning rate approach in analogy to Caldera at el. [50] has been implemented, assuming a constant learning rate (LR) of 15 % [33]. The potential future $capex_{new}$ can be calculated based on the prototype $capex_{initial}$ via Eqs. (21)-(23). In this study, a projected production volume of approx. 1 Mt of $CO_2$ per year capture capacity is assumed, which equals 30,000 standard units, a common scale up magnitude [13,52]. The exponential growth factor *b* in Eq. (23) can be obtained by Eq. (22), via the progress ratio *PR*, which in turn is given by Eq. (21). [50]

$$LR = 1 - PR \tag{21}$$

$$PR = 2^{-b} \tag{22}$$

$$capex_{new} = capex_{Initial} \cdot \left( \frac{production_{new}}{production_{initial}} \right)^{-b} \tag{23}$$

### 2.4. Limitations and assumptions of the model

As with every model, the one provided in this work does rely on certain assumptions and has certain limitations. For a packed bed with such large diameter/ length to particle size ratios, a 1-D model with phases in thermal equilibrium is generally accepted as sufficiently accurate [53–55]. Effects such as bypass streams due to bed inhomogeneities, must be analysed before practical implementation, but are out of scope for this study. The due to the large size of the bed, the rather small outer surface in respect to the volume does justify adiabatic behaviour in this scope, however especially the steam desorption will suffer from heat loss in a practical application. This also applies to the steam cycles, which deliver a valid indication of feasibility and a general order of magnitude for energy consumption, but will need further engineering, before a practical implementation. The ideal mixing of air inside the building can be reasonably assumed, because there is a central duct collecting the exhaust air. Even with an irregular distribution of inhabitants, the average across the building is represented by the exhaust concentration. However, for a real implementation, the individual building has to be analysed.

## 3. Results and discussion

### 3.1. Operational parameters of the standard adsorber unit

As mentioned (Section 2.1), a standard unit was defined consisting of two packed bed adsorbers in parallel, each with a diameter of 3 m and a length of 0.8 m to achieve a pressure drop below 150 Pa (146 Pa, according to Eq. (6)) at the design nominal throughput of $\dot{V}_{air,nom}$ of 11,000 $m^3h^{-1}$ each, summing up to the 22,000 $m^3h^{-1}$ total throughput of the standard unit.

Optimal operation parameters can be deduced from the adsorption kinetics, predetermining at what point in time the regeneration is to be initiated.

Fig. 2a shows the $CO_2$ concentration of the gas phase ($\dot{V}_{air,nom}$) as a function of time and the adsorber length. Due to the high volumetric flow rate and low inlet concentration, strongly pronounced breakthrough phenomena as known for other TPSA applications do not occur. The temperature in the adsorber is relatively constant during the adsorption, if the adsorber starts in thermal equilibrium. The maximum temperature increase due to heat of adsorption of $CO_2$ and water was found to be less than 5 K (see SI, Fig. S5). Using the outlet concentration data obtained, capture efficiency $\eta_{Cap}$ (Eq. (1)), i.e. the proportion of captured $CO_2$ from the air can be plotted over time: Fig. 2b shows $\eta_{Cap}$ at nominal and reduced flow rates as a function of adsorption time. It is obvious, that a lower flow rate results in higher capture efficiency, but it

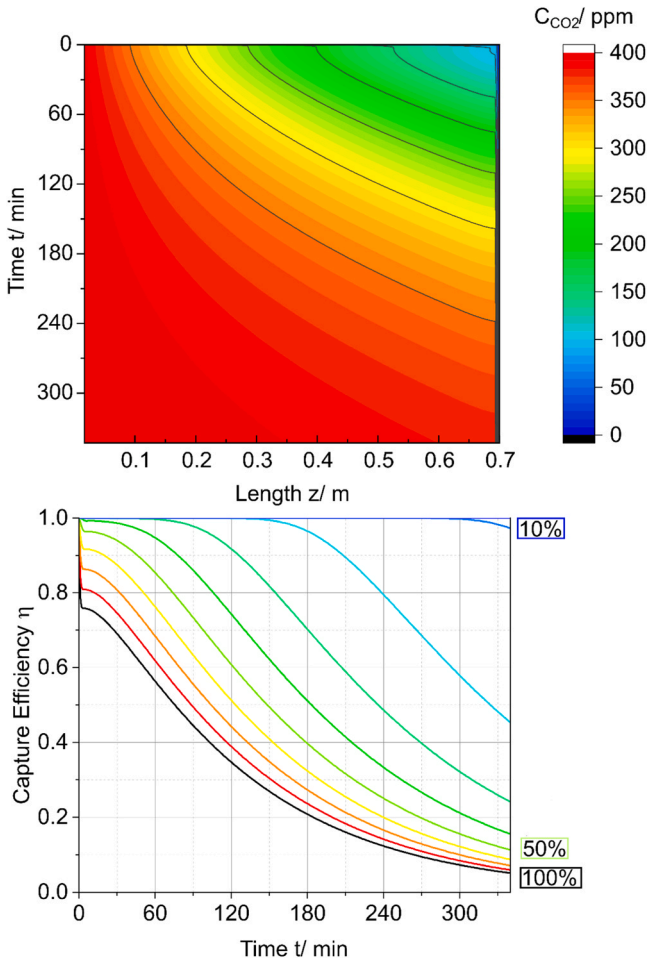


**Fig. 2.** (a) Temporal and spatial concentration profile in the adsorber bed during adsorption at nominal air flow rate. (b) Capture efficiency over time at varying air flow rates in 10 % increments (percentage of nominal flow rate $\dot{V}_{air,nom}$ = 11,000 $m^3h^{-1}$ through each adsorber of the standard unit).

is noteworthy mentioning that only below 40 % nominal flow rate, an efficiency of 100 % can be achieved at all. At nominal flow rate, $\eta_{Cap}$ starts at around 70 % and then continuously decreases to lower values over time.

Therefore, the earlier the DAC is switched from adsorption to desorption mode, the higher the average capture efficiency. To achieve the predefined criterion of at least 50 % average capture efficiency (see Section 2.1), for nominal air flow rate the critical efficiency $\eta_{cap,crit}$ defining the switch from adsorption to regeneration is at 35 % resp. after 120 min resulting in an average capture efficiency $\eta_{cap,av}$ of 57 %. It could prove beneficial to run the adsorption for a longer period of time, yielding a higher average loading $q_{CO2}$, with reduced capture efficiency to reduce the thermal energy demand while regenerating by increasing the ratio of bound $CO_2$ to inert material, which has to be heated in any case independent of the loading. Therefore, for the nominal air flow rate, a critical capture efficiency $\eta_{cap,crit}$ of 5 % representing a very high loading $q_{CO2}$ after a capture time of 340 min resulting in $\eta_{cap,av}$= 30 % was also considered in this study to assess the performance of the system.

After the defined $\eta_{cap,crit}$, has been reached, the desorption phase is initiated by stopping the air flow before the pressure in the sorption chamber is decreased: For the evacuation, the total gas volume $V_{gas,chamber}$ within the adsorber incl. peripherals and the porous adsorbent must be removed by the vacuum pump. In order to also consider additional dead volume of the piping etc., in this study a total gas volume of $V_{gas,DAC,tot} = 2\ V_{gas,chamber}$ was assumed. Evacuation is performed by the vacuum pump with a constant volume flow rate of 1200 $m^3\ h^{-1}$ at eventually 0.1 bar(a). After evacuation a constant mass flow rate of steam (0.6 kg $s^{-1}$) is fed to ensure sufficiently fast regeneration.

Fig. 3 shows the $CO_2$ outlet concentration (a) and the spatial and temporal temperature distribution (b) over time of desorption. Initial evacuation to reach 0.1 bar(a) takes only approx. 2 min and therefore is not directly recognizable in Fig. 3a and b. After reaching 0.1 bar(a), steam at 100°C/0.1 bar(a) is injected. Qualitatively, there are three distinct regions of changes in $CO_2$ output concentration during the desorption step (Fig. 3a): Region I (until approx. 52.5 min in Fig. 3a) is caused by the decrease in pressure and rise in temperature due to the adsorption of water (steam), the increase in temperature in that region can also been seen in Fig. 3. The second region (52.5 min to 60 min) is initiated by the heat front approaching the end of the adsorber bed. At this point in time the whole bed is heated evenly, and the desorption process accelerates again. To ensure that the desorption process is kept running until the unit is heated completely, for the $CO_2$ outlet concentration a threshold value of 0.0015 $mol_{CO2}\ m^{-3}$ is defined.

Once the threshold concentration is reached, the system is cooled down by injecting 45°C saturated steam until $T \leq 60°C$ is given throughout the adsorber bed, to prevent excessive oxidation. Due to the sudden drop in temperature and therefore increase in gas density, the $CO_2$-concentration drops to near zero for the process of cooling (region III in Fig. 3a).

### 3.2. System simulation

#### 3.2.1. Influence of the intake air properties

Intake air conditions, mainly temperature and humidity, certainly has an effect on sorption characteristics. As outlined in Section 3.1 one key source of heat in the desorption process is the heat of adsorption of water. The water contained in the air will readily adsorb during the capturing step which should promote $CO_2$ capture on the one hand, but

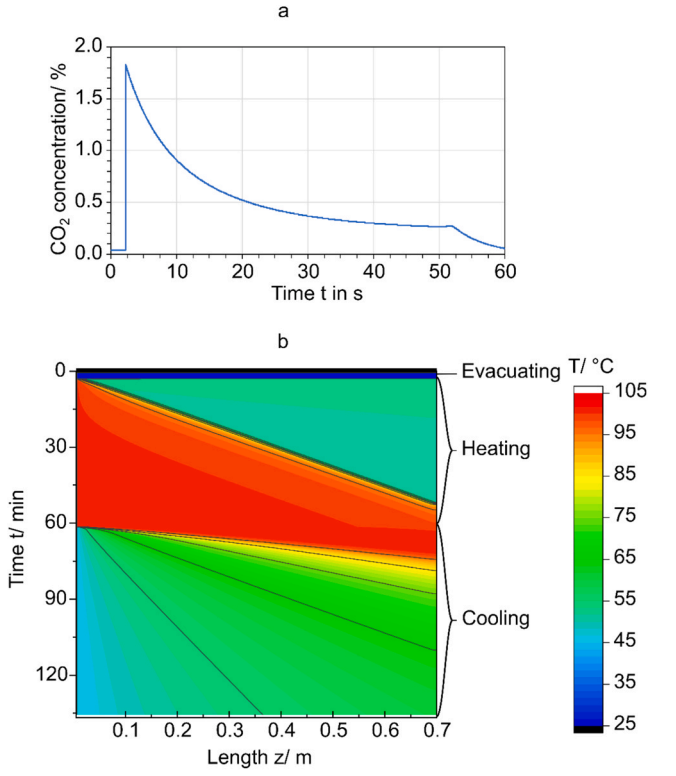


**Fig. 3.** (a) $CO_2$ output concentration for the desorption process at 0.1 $bar_{abs}$, 100°C. (b) Spatial and temporal temperature distribution during the desorption step.

also increase the thermal energy demand during regeneration since less water can adsorb from steam. Therefore, the influence of the relative humidity $\varphi$ has been studied for a constant temperature of 20°C and $\eta_{cap,crit}$= 5 %. For the uncontrolled ventilation the results are shown in Fig. 4. As expected, the energy demand decreases drastically with decreasing relative humidity and more than halves from ϕ= 90–10 %. The capture rate (shown in kg $CO_2$ captured within 48 h) on the other hand stays relatively constant. However, a maximum can be found for medium ϕ, which can be assigned to the counteracting effects of the relative humidity on $CO_2$ capacity and desorption time.

Another aspect often associated with operating a DAC is the co-capture of water. As mentioned before, not only $CO_2$ but also water vapor from the air sticks to the sorbent material, so in theory water can

be captured as a byproduct. On the other hand, while regenerating, water also adsorbs to the material and is lost, when switching back to the capture step. The data show, that below a relative humidity of 70 %, water is lost in the operation of the DAC, while the net water balance is positive if the air is more humid. At ϕ= 90 % the mass of water that can be captured is three times that of $CO_2$, which means that on a molar basis the ratio is around 1.2. This water could be used as a product resp. feed for e.g. water electrolysis (relevant in the P2X context) and/or recycled to replenish water demand of the DAC plant. Most water is lost after regeneration, when air is pushed through the bed, carrying out the still adsorbed water from the steam.

To check for effects on a more practical level, for the same scenario as above temperature was varied over the day by a diurnal variation explained in the SI chapter 1.4 with an amplitude of roughly 10 K. The humidity has been kept constant at ϕ= 10, 40, 80 % according to the following five cases representing rather extreme climate conditions to showcase the trends:

- Hot and dry, e.g. desert: $T_{Base}$ = 25°C, ϕ= 10 %
- Hot and humid, e.g. tropics: $T_{Base}$ = 25°C, ϕ= 80 %
- Moderate climate conditions e.g. Germany in spring and fall: $T_{Base}$= 10°C, ϕ= 40 %
- Chill and humid climate, e.g. northern coastal region: $T_{Base}$= -5°C, ϕ= 80 %
- Cold and relatively dry, Arctic: $T_{Base}$ = -5°C, ϕ= 10 %

It can be seen (Fig. 5), that the dry cases benefit from significantly lower energy consumption, which is consistent with the result above. The temperature of the intake air seems to play a minor role on the thermal energy demand. The capture capacity on the other hand shows significant reductions with an increase in temperature: it decreases almost by 60 % when comparing a base temperature of −5°C to 25°C. This would mean, that locations with dry and cold conditions would provide ideal operation conditions for the DAC system.

These results can also be transferred to standalone DAC systems, since it does not make any difference if the DAC is connected to a ventilation system or not. However, for HVAC-coupled systems these

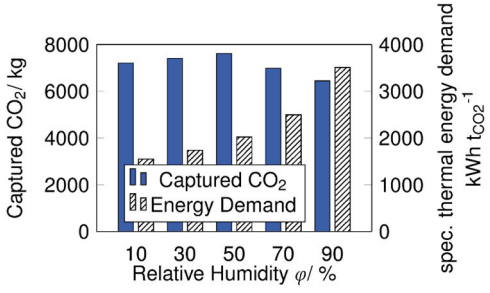


**Fig. 4.** Thermal energy consumption and mass of captured $CO_2$ within 48 h of the intake DAC at different relative humidities of the air for, $\eta_{Cap,Crit}$= 5 %, T = 20°C and uncontrolled ventilation at nominal flow.

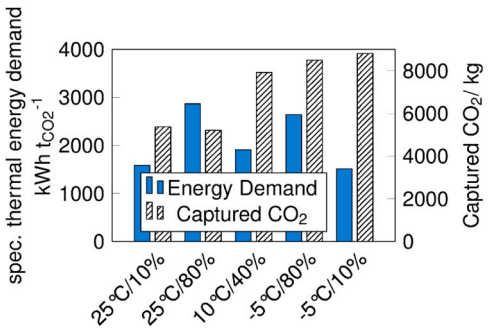


**Fig. 5.** Thermal energy consumption and mass of captured $CO_2$ within 48 h of the intake DAC at different climate conditions of the air for, $\eta_{Cap,Crit}$= 5 %, diurnal temperature variation from base Temperature and uncontrolled ventilation at nominal flow.

results are in particular interesting as intake air properties are also dependent on the implementation scheme: If the DAC is installed in the intake stream of the HVAC system, it is sensible to position the DAC upstream the heating unit to ensure lower temperatures, but downstream the AC if the air is cooled down. In addition, AC-systems often dehumidifies the air. Given the fact that the spec. thermal energy demand decreases with decreasing humidity (see Fig. 4), the DAC unit should be placed downstream a dehumidifier if there is any. If the DAC is placed in the exhaust stream it should be placed downstream a possible heat recovery system, as temperatures and possibly relative humidities are lower here. Seasonal variations in humidity could be accounted for by using valves in the ducting to position the DAC in the dryest part of the system. In winter this could be after heating, while in summer this is usually directly in the intake, as cooling increases the relative humidity.

### 3.2.2. *Influence of the operation parameters*

Another way to influence the performance of the DAC is to alter the operating conditions. The first metric investigated is the cutoff criterion $\eta_{Cap,Crit}$, defining the point in time when to switch from capture to regeneration. The shorter the capture step, the less $CO_2$ is adsorbed on the one hand, but

the total cycle time decreases on the other hand. For that matter all three building types have been simulated for an exhaust air DAC with the two $\eta_{Cap,Crit}$, defined in Section 3.1 (5 %, 35 %). The results are shown in Fig. 6. With increasing occupancies (WH → OB → OPO), the energy consumption almost stays constant while the capture rate increases, e.g. for WH vs. OPO by about 14 % for $\eta_{Cap,Crit}$= 5 % and by 14 % for $\eta_{Cap,Crit}$= 35 %. The shorter cycle times of the scenarios with $\eta_{Cap,Crit}$= 35 % lead to a 20 % increase in capture capacity on average which however requires approx. 26 % more thermal energy. Due to the higher capture capacity, the electrical energy demand drops by 61 %,

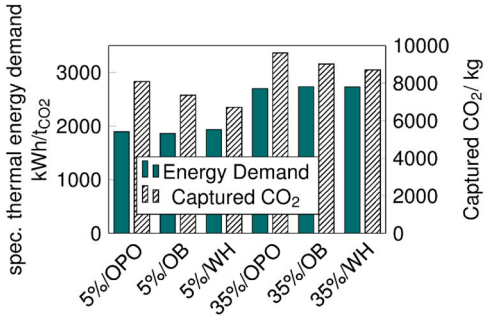


**Fig. 6.** Thermal energy consumption and mass of captured $CO_2$ within 48 h dependent on the minimal capture efficiency $\eta_{Cap,crit}$ for the various buildings (uncontrolled ventilation, constant temperature and humidity. (T = 20°C, φ=40 %)).

because energy for the fan stays roughly constant. This leads to the conclusion, that most of the heat is required to warm the inert materials and not driving the desorption reaction. Materials with high(er) capture capacity are therefore key for further reducing the energy demand.

As discussed above, the capture rate in an uncontrolled ventilation scenario has only a limited effect on the energy demand (compare Fig. 6). To determine potential improvements in efficiency, PID controlled ventilation of the buildings was implemented into the simulation (same cases). The increased average $CO_2$ concentration could decrease the spec. thermal energy consumption. The results shown in Fig. 7 reveal, that the further increase in $CO_2$ concentration (to 700 or 1000 ppm) does influence the energy demand.

The average thermal energy demand for the three scenarios with uncontrolled ventilation is 1845 kWh $t_{CO2}^{-1}$, whereas the two cases with setpoint 700 ppm and 1000 ppm require on average 1656 kWh $t_{CO2}^{-1}$ and 1529 kWh $t_{CO2}^{-1}$ respectively. Here, a clear reduction in thermal energy demand is noticeable, at otherwise similar operating conditions. The electrical energy demand decreases even more, since the average volume flow is much lower reducing the pressure drop and therefore also the power demand to 35 kWh $t_{CO2}^{-1}$ (700 ppm) resp. 11 kWh $t_{CO2}^{-1}$ (1000 ppm). (compare SI, Table S5) It is interesting to note here, that the energy demand is higher in the cases of the higher occupied building (OPO) as for the controlled ventilation system, the required volume flow rate needed to keep the $CO_2$-concentration low (according to the control setting) is higher the more people generate $CO_2$ in the building.

In addition, data shows (SI Figure S6) that the axial $CO_2$ gradient in the adsorber bed is smaller the higher the air flow rate, i.e. the higher the occupancy of the building in the controlled ventilation scenarios. Therefore, the capture efficiency is lower and the adsorber on average not as saturated as with low volume flows at SP= 700 ppm. Here (700 ppm) a rather sharp front of saturation moves through the adsorber. The regeneration is therefore introduced at a rather high average loading, even though the average intake $CO_2$ concentration is lower, compared to a higher occupancy scenario. The capture capacity for the controlled ventilation scenarios is vastly lower than for an uncontrolled system. The DAC almost exclusively captures $CO_2$ produced by the occupants in the building, also explaining why the same buildings have similar captured mass of $CO_2$ per time, although based on different threshold setpoints. All in all, it could be shown, that energy efficiency can be improved by the control strategy however, on cost of capture capacity.

In addition to economic or performance aspects, the ventilation strategy must also consider other boundaries, such as air quality and regulation. Although the setpoints are chosen in respect to applicable law, in real-world application the operation of the HVAC must make sure to always meet the criteria, even with fluctuation in the system. Additional sensors or a more complex control scheme could be necessary. The wrong choice of cycle times and ventilation rates can lead to overshoots and periods of bad air quality and must be kept in mind, when designing the system. Apart from $CO_2$ the humidity must be accounted for, as directly after regeneration moisture is expelled from the unit, which either has to be removed by the AC's dehumidification or deliberately injected into the building as a means to increase humidity, when the air is too dry.

Since the regeneration is the energy intensive step, a possible option to save energy is to lower the heating power, so that the Adsorber is heated at a lower rate and more evenly, which could avoid unnecessary energy input, because the time for $CO_2$ desorption/diffusion is increased. However, results show (Fig. 8), that a heating power reduced to 10 % (i.e. 6 kW per module compared to 60 kW on average) does not decrease the specific heat demand significantly. This is due to the fact that the regeneration time triples in that case and the capture capacity drops drastically. One benefit however would be, that the evaporator unit can be engineered smaller eventually reducing capex. In a real system due to the substantially higher desorption time, it is likely there will be far higher heat losses of the overall system, leading to ever higher net energy demands, which makes this approach not useful in terms of energy saving. Nevertheless, it will be included in the TEA (Section 3.3).

### 3.2.3. Heat storage dimensions

With a peak power consumption of 60–70 kW, depending on the specific scenario, for one module, the solar thermal unit with its 35 kWp is never able to power the DAC directly. Therefore, grid energy or a heat storage is required. In the previous considerations, the heat storage was not interfering with the DAC operation, ergo grid energy was used, when the storage was empty. In this study, the heat storage level directly influences the DAC by prohibiting the switch from adsorption to regeneration as long as there is not enough energy to fully execute that step. At first, a storage capacity great enough to sustain uninterrupted operation has been implemented. It was found, that a capacity of more than 120 kWh enables continuous operation and energy demand and capture rate are similar as when the storage is not taken in account, at least for $\eta_{Cap,Crit}$= 5 %. In case of the higher $\eta_{Cap,Crit}$= 35 % the capture rate did drop approx. 20 %. In Fig. 9a, the timeline of stored energy is shown for one unit. One regeneration cycle only needs around 40 kWh of energy, which is why a smaller capacity of 45kWh was investigated to ensure that one cycle is possible on one charge with a certain safety margin. The timeline is shown in Fig. 9b.

The performance data for the case of 45 kWh storage is shown in Fig. 10. It can be seen, that compared to the unrestricted DAC system the overall capture capacity decreases by a factor of approx. 2.

Additionally, it is noticeable, that the differences between $\eta_{Cap,Crit}$= 5 % and 35 % diminished as here the stored energy is the limiting factor and therefore responsible for defining the point in time for the transition from capture to regeneration step. From the economic point of view, in this case it could be beneficial to use grid energy if available to

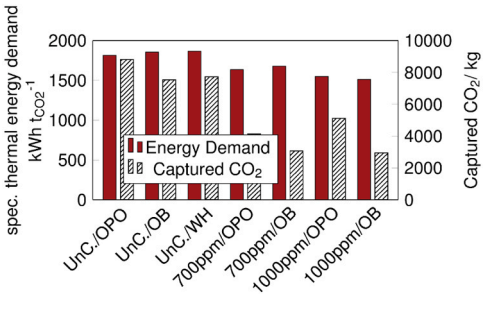


**Fig. 7.** Thermal energy consumption and mass of captured $CO_2$ within 48 h for scenarios with PID-controlled (constant $CO_2$ concentration) versus uncontrolled ventilation. Data are shown for different minimal capture efficiency $\eta_{Cap,Crit}$ for the various buildings (constant temperature and humidity. (T = 20°C, φ=40 %), variable setpoint for $CO_2$ concentration).

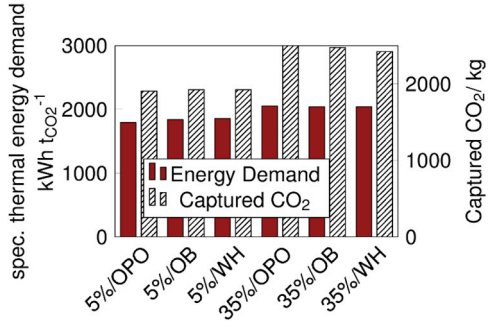


**Fig. 8.** Thermal energy consumption and mass of captured $CO_2$ within 48 h for scenarios with heating capacity decreased to 10 %. Data are shown for different minimal capture efficiency $\eta_{Cap,Crit}$ for the various buildings (uncontrolled ventilation, constant temperature and humidity. (T = 20°C, φ=40 %).

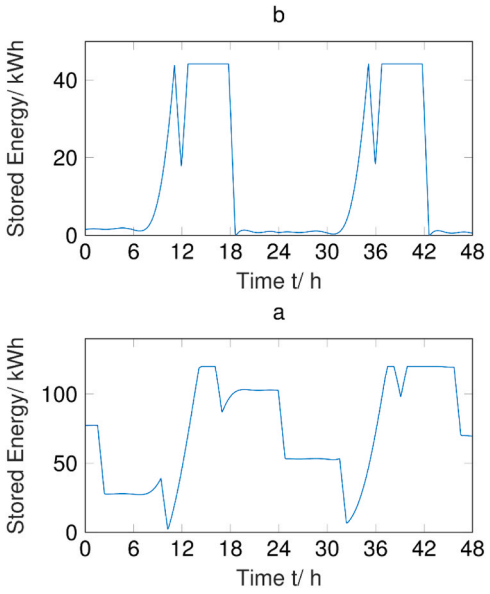


**Fig. 9.** Progression of energy stored in the heat storage for exhaust DAC in the office building (OB) at nominal air flow rate, $\eta_{Cap,Crit}$= 5 %. (a): heat storage capacity of 120 kWh, and (b): 45 kWh.

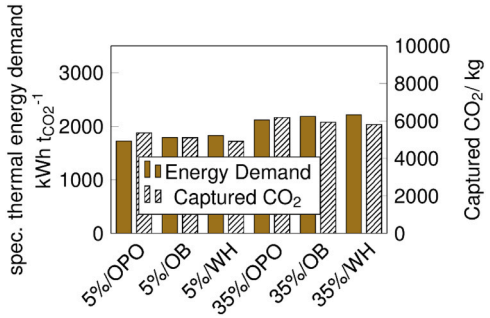


**Fig. 10.** Performance of the DAC with a limited heat storage capacity of 45 kWh with the same scenarios as in Fig. 6 with uncontrolled ventilation, various buildings and constant temperature and humidity. (T = 20°C, φ=40 %).

keep the capture rate high and thus capture more of the "product" $CO_2$. The trend of stored energy also shows that following the predefined restrictions in the simulation study the DAC cycles for the small energy storage (Fig. 9) only occur regularly during daytime, when the storage is replenished by the solar thermal plant and basically come to a standstill in the night. This also illustrates that the DAC unit is restricted by the energy input.

### 3.2.4. DAC via an alternative adsorber material Lewatit VP OC 1065

The results discussed so far are based on the nano-cellulose material, which has beneficial properties, especially regarding the high porosity and therefore low pressure drop combined with high amine density. This gives a viable look into the future of DAC technology. However, to draw a picture on how such a system would work and look like with a currently available adsorber material, properties of Lewatit VP OC 1065, being commercially available, was implemented in the DAC model. Compared to nano-cellulose-based sorbent, the amine functionalized ion exchange resin from Lanxess has very different properties, with the major difference being that Lewatit is a much more compact material, limiting mass transport and increasing pressure drop, see also summary of the data on physico-chemical properties taken from Young et al. and the data sheet from Lanxess [17,37] in Tables S2 and S3.

In order to fulfill the same criteria as defined for the nano-cellulose material (Section 2.1), an adsorber based on the same available space restrictions for construction (two times 3 ×0.7 m) was designed: it uses concentric rings with a much smaller bed length of 1.5 cm, but a 4.13 times larger intake surface area. The flow of air is radial through the bed. The construction is shown in Fig. 11a. This design allows for a pressure drop of only 97 Pa at nominal flow rates and an average capture efficiency of 49 % can be achieved at $\eta_{Cap,Crit}$= 35 %.

With the modified adsorption isotherms and the bed design described above, the same simulations

have been run as for the nano-cellulose system with uncontrolled ventilation, varying $\eta_{Cap,Crit}$, T = 20°C, ϕ= 40 % and for the three buildings (cf. Fig. 6).

As can be seen in Fig. 11b, the performance of Lewatit is comparable to the nano-cellulose system with a maximum increase of capture capacity of 20 %. The nano-cellulose shows less specific thermal energy demand than the Lewatit adsorber (at $\eta_{Cap,Crit}$=5 %), by 7–19 %. For $\eta_{Cap,Crit}$= 35 %, thermal efficiency of the Lewatit system is approx. 0–3 % higher. This is due to the fact that the short bed results in a more constant loading profile, so the effect of unequal loading occurring at short cycle times is less pronounced. At full loading in comparison to the nano-cellulose material requires less thermal energy due to less mass of inert material. The electric energy demand of the two systems is likewise very similar. In summary, both materials have their merit, and the decision which sorbent (and consequently which design of the adsorber) is to be used could and should be made based also on other metrics such as material availability, costs and lifetime. The simpler construction of the nano-cellulose bed as of now would favor this material from the economic point of view.

### 3.2.5. Steam cycle

For the nano-cellulose material, different steam cycles explained in Section 2.2.9 have been analyzed in terms of thermal energy demand. The results are summarized in Table 1. When implementing a heat pump to raise the temperature from condensation to evaporation the amount

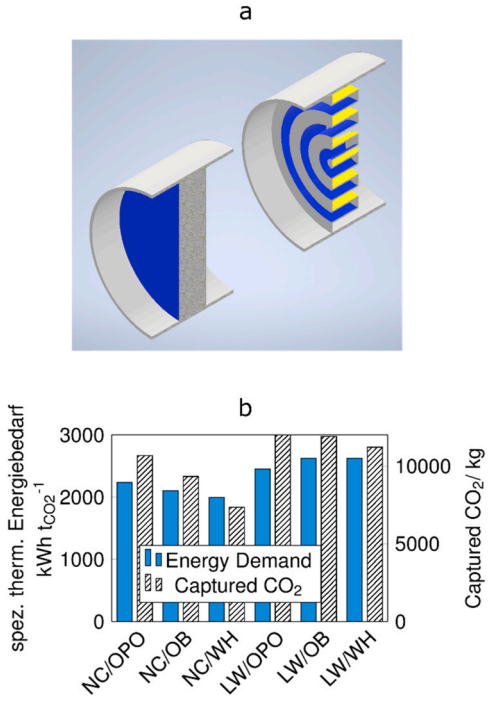


**Fig. 11.** Alternative concept of DAC using Lewatit as a sorbent material. (a) Design of the adsorber bed for Lewatit (right) and for nano-cellulose (left), (b) thermal energy consumption and mass of captured $CO_2$ within 48 h for $\eta_{Cap,Crit}$ = 5 % for the various buildings (uncontrolled ventilation, constant temperature and humidity (T = 20°C, φ=40 %)).

**Table 1**
Comparison of the ideal calculation for the thermal energy consumption and the engineered steam cycle for the case.

| Build. | $\eta_{Cap,Crit}$ | Exhaust Compression | | Heat Pump | | Ideal | |
|---|---|---|---|---|---|---|---|
| | | Therm. | Elec. | Therm. | Elec. | Therm. | Elec. |
| - | % | kWh $t_{CO2}^{-1}$ | | | | | |
| **WH** | 5 | 836.2 | 1561.6 | 1976.1 | 16340.2 | 1866.2 | 245.7 |
| **OB** | 5 | 1002.6 | 1827.9 | 2367.5 | 19528.4 | 1854.43221 | 251.8 |
| **OPO** | 5 | 864.4 | 1571.1 | 2035.6 | 16782.7 | 1813.1 | 216.9 |
| **WH** | 35 | 1182.5 | 2153.4 | 2928.1 | 24372.4 | 2536.3 | 165.1 |
| **OB** | 35 | 1175.3 | 2093.8 | 2889.8 | 23866.1 | 2519.5 | 156.4 |
| **OPO** | 35 | 1000.0 | 1803.9 | 2466.5 | 22314.1 | 2461.7 | 145.6 |

of heat moved from condensation to evaporation is too large for a sensible operation. Between 17 and 25 MWh of electrical energy per ton of $CO_2$ would be needed to run the heat pump. Thus, this operation scheme is economically not feasible. However, the results show an interesting alternative operation mode: Since most energy is needed for evaporation which takes place at only 45°C, waste heat streams of very low temperature could be tapped here. Although the temperature is low, the amount of heat is still substantial. Therefore, such scenarios would apply mainly to industrial settings. There are studies suggesting a significant resource of untapped waste heat, especially at relatively low temperatures, that could this make possible [56]. In that case, only the energy for superheating would be required, which is in the range of 2000–3000 kWh $t_{CO2}^{-1}$, so in good proximity to the idealized results from Fig. 6. The scheme with exhaust steam compression shows, that a smart heat recovery system can be engineered to sufficiently lower the energy demand. Here, most energy is needed for said compression within a range of 1400–2000 kWh $t_{CO2}^{-1}$. Additionally, around 1000 kWh of thermal energy is needed for superheating, which is actually lower than in the idealized scenarios. These results underline the importance of a clever heat integration with which efficient operation is feasible.

### 3.3. Techno economic assessment

With Direct Air Capture, especially when comparing to $CO_2$ capture from higher concentrated sources (e.g. industrial point sources), cost is one of the most important aspects predetermining broad implementation. The usual measure is the levelized cost per ton of $CO_2$ captured (here: Levelized Cost of Direct Air Capture, LCOD). To assess the performance of a single HVAC integrated DAC unit a TEA has been conducted.

#### 3.3.1. Assumptions and considered scenarios

The capital expenditures (capex) have been determined, wherever possible based on quotations/information of web-shops of commercial suppliers for the following major components including all associated cost and by applying the Lang-Factors summarized in Table S4 in the SI:

- Vacuum vessel: To handle the regeneration, a vessel capable of operating at 0.1 bar absolute has to be designed according to AD2000 and a steel price of 600 € per ton has been assumed [57].
- Fan: Two offers from a commercial supplier have been taken for a fan that is able to handle (a) the whole 22,000 $m^3h^{-1}$ at 500 Pa pressure drop, to handle the DAC and the building HVAC, for the standard case resp. (b) for lower volumetric flow rates at 200 Pa pressure drop to be used in scenarios with controlled ventilation and lower resulting pressure drop.
- Vaccum pump: The vacuum pump has been dimensioned to handle 1200 $m^3h^{-1}$ at 0.1 bar (see Section 3.1)
- Adsorber material: Given the fact that there are no data available for the nano-cellulose system, Lewatit material was used for assigning the cost for the filling.
- Evaporator: Offer of a commercial supplier for a boiler with heating capacity of 66 kW as in the simulation a maximum heating power of 60–70 kW has been identified.
- Since the unit is of low TRL and some components are not included in the cost-estimation (e.g. vacuum doors, heat exchangers, etc.) a rather large lang-factor of 3.9 has been assumed for parts, that need further assembly and auxiliaries.
- Similar to Fasihi et al. [33] the fixed operational expenditures (opex) have been set at a constant percentage of 3.7 % of the capex.
- For the capex reduction via future mass fabrication, a constant learning rate of 13 % with an increase to eventually 30'000 units in total is assumed. This would equate to an integral capture capacity of 1 Mt of $CO_2$ per year, which is the scale most DAC companies stride to [14].
- For energy cost (opex), 0.06€ per kWh have been assumed for both heat and electricity, which is an estimate for the generation cost of PV-power in the near future [58]. Additionally, a general 30 % increase in $CO_2$-loading-capacity ($mol_{CO2}$ per kg of sorbent material) due to expected adsorber material improvements has been assumed for all cases.
- For all cases with people within the building (i.e. OB and OPO) it is assumed, that people are only present at workdays and not at weekends, where the building remains empty.
- The following scenarios S1-S10 have been investigated (all for $T = 20°C$ and $\phi$=40 % air):

  - S1: WH with $\eta_{Cap,Crit}$= 5 % and uncontrolled ventilation
  - S2: OB with $\eta_{Cap,Crit}$= 5 % and uncontrolled ventilation
  - S3: OPO with $\eta_{Cap,Crit}$= 5 % and uncontrolled ventilation
  - S4: WH with $\eta_{Cap,Crit}$= 35 % and uncontrolled ventilation
  - S5: OB with $\eta_{Cap,Crit}$= 35 % and uncontrolled ventilation
  - S6: OPO with $\eta_{Cap,Crit}$= 35 % and uncontrolled ventilation
  - S7: OB with $\eta_{Cap,Crit}$= 35 %, uncontrolled ventilation free waste heat at 100°C (i.e. no cost for thermal energy assumed)
  - S8: OB with $\eta_{Cap,Crit}$= 35 % and controlled ventilation at setpoint 700 ppm (smaller, i.e. cheaper fan installed)
  - S9: OB with $\eta_{Cap,Crit}$= 35 % and uncontrolled ventilation with exhaust steam compression cycle (considered via double cost for vacuum pump to account for compressor)
  - S10: OB with $\eta_{Cap,Crit}$= 35 % and uncontrolled ventilation with steam cycle and free heat at 50°C (only thermal energy demand for superheating).

#### 3.3.2. Results of the TEA

The results of the techno-economic assessment are summarized in Fig. 12. It can be seen, that the capex is the main driver of the LCOD even with the learning rate approach, followed by the energy costs. This is why the cases with a large occupancy (OB, OPO) show significantly lower LCODs, although as shown earlier the specific energy demand is not affected a lot while the increase in $CO_2$ concentration (respiration of the people) results in an increase of the overall capture rate. Similarly, the scenarios with controlled ventilation show a lower capture rate and therefore a higher LCOD, because less air is pushed through the adsorber. The capex reduction due to the smaller fan cannot compensate that trend. In general, the cost found at the lower end of the assessment match those of other TEAs in literature with S7 being the lowest at 280 € $t_{CO2}^{-1}$ because of the free energy assumed. For the reference scenario (S1)

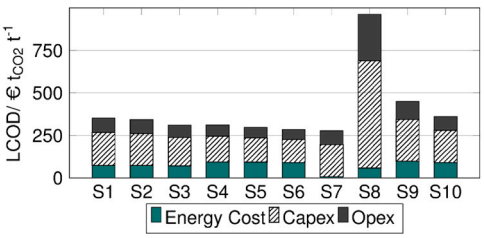


**Fig. 12.** Techno economic assessment of the DAC standard unit: LCOD for the $CO_2$ of the HVAC integrated DAC plant for different types of buildings (OB, OPO, WH) and different control and heat integration strategies. For details on S1-S10, see Section 3.3.1.

LCOD are 354 € $t_{CO2}^{-1}$, with a decrease to 313 € $t_{CO2}^{-1}$, when increasing the occupancy (S1 (WH)->S2 (OB)->S3 (OPO)). Interestingly, $\eta_{Cap,Crit}$= 35 % results in lower LCOD as compared to $\eta_{Cap,Crit}$= 5 %. The reason is again the higher capture rate impacting the LCOD more than the increased spec. energy demand for shorter cycles. All LCOD are still remarkably higher than the targeted costs claimed by most DAC companies, that run around 100 € $t_{CO2}^{-1}$ [13,32,33]. To reach those numbers, further improvements at the adsorber that boost the capacity and mass fabrication for even lower capex would have to be implemented. The steam cycle cases (S9, S10) also show, that a much smarter way of integrating the heat in the process is necessary to achieve low costs as it is not granted to always have enough free waste heat to run the process. The scenarios with a steam cycle (S9, S10) do show higher LCODs between 363 and 453 € $t_{CO2}^{-1}$ respectively. These costs are higher due to the increased energy demand and capex, but even when hypothetically including additional energy losses, LCOD below 450 € $t_{CO2}^{-1}$ should be doable. This cost would be in the range of other scientific literature on economic assessments of DAC, showing that our models results are comprehensive [31,33,59].

There is one interesting mode of operation, if at least three units are installed at the site. With S2 as a basis, the data show, that the adsorption step requires twice the time of the regeneration step. Therefore, one steam generation unit can be used to feed the three units. The capex of the steam related components then drops by 66 % and the capex of the fan by 33 %. With these alterations the cost of DAC can be reduced to 271 € $t_{CO2}^{-1}$ even with the higher costs for heat supply.

Apart from the already discussed contributions to the economics of the HVAC/DAC-System, a real-world implementation would be accompanied by further complications. The increased complexity would require additional maintenance, especially as the sorbent has to be renewed in periodic intervals and the $CO_2$ must be handled. In this work, maintenance efforts are accounted for by a fixed Opex, but the complexity of such a system, or $CO_2$ infrastructure in general (pipelines, trucks etc.) are hard to quantify and should be considered in future works.

Fasihi et al. [33] did a techno-economic review based on data available from companies or literature and concluded a LCOD of US$ 222 (204 € $t_{CO2}^{-1}$) for "today" and predicted US$ 54 (50 € $t_{CO2}^{-1}$) for the year 2050, both per ton of $CO_2$. With a currency exchange ratio of 0.92 € per USD this equates to 50–204 € $t_{CO2}^{-1}$. They however did not perform own estimates for capex and assumed a lower capex per capture rate of 730 € $t_{CO2}^{-1}a^{-1}$ based on an estimate by Antecy [60]. In our work the capex per production capacity (Euro per yearly capture capacity) in the future scenario ranges from 1586 to 7368 € $t_{CO2}^{-1}a^{-1}$ depending on the case. Additionally, they assumed free waste heat. Lackner and Azarabadi [61] postulated a current LCOD of US$ 500 $t_{CO2}^{-1}$ (460 € $t_{CO2}^{-1}$) and assume, that the goal of US$ 100 $t_{CO2}^{-1}$ (92 € $t_{CO2}^{-1}$) can be reached in the future, assuming a substantial ramp up in the production capacity leading to a substantial decrease in installation costs. Sievert et al. [59] calculated the cost of DAC to reach US$ 226–544 $t_{CO2}^{-1}$ (208–500 € $t_{CO2}^{-1}$) for solid sorbent DAC units in a novel cost-projection method they developed. This would fit to the data of the present study. Sabatino et al. [31] analyzed various DAC technologies and draws the conclusion, that LCOD below US$ 200 $t_{CO2}^{-1}$ (184 € $t_{CO2}^{-1}$) are achievable with all major DAC technologies, including LT-DAC, which is also in accordance to the findings discussed in the present contribution. Apart from cost, the specific energy demand (both thermal and electric) in the above-mentioned studies is comparable to our findings.

## 4. Conclusions

Large DAC capacities are required to meet the goals agreed on in the Paris Agreement. Therefore, every possibility to ensure a rapid increase in capture capacity should be taken and each opportunity of improvement is viable to the future of the field. In this paper, it is shown that the integration of DAC modules into (also existing) ventilation systems can be beneficial to the operation of DAC plants. The elevated $CO_2$-concentration given by the respiration of people within the building results in lower thermal energy demand of the DAC unit. If the $CO_2$ level is increased from the ambient 400–1000 ppm, for a $CO_2$-concentration controlled ventilation system, the thermal energy demand can be reduced from roughly 2000 kWh $t_{CO2}^{-1}$ to less than 1600 kWh $t_{CO2}^{-1}$. The humidity of the air has been identified as important parameter as capture capacity increases with humidity while also resulting in a higher thermal energy demand, when regenerating with direct steam injection. Low temperatures of the intake air on the other hand promote $CO_2$ adsorption. Concerning the sorbent material, Lewatit has been found to perform similar compared to nano-cellulose (based on sorption kinetics), but requires a more complex design of the adsorber in order to also guarantee low pressure drop. The integration of a heat storage of approx. 120 kWh can enable the DAC unit to run continuously with a solar thermal field of 35 kWp, but energy losses in a real-world application would lead to a higher energy demand and therefore require a grid connection or other heat sources. The increase in occupancy and therefore $CO_2$ concentration increases the capture rate, which reduces the LCOD, as the capex is still the major driver of the LCOD. From an empty building (warehouse in this study) to a densely populated office space, the LCOD can be reduced from 352 to 310 € $t_{CO2}^{-1}$. Energy cost also quite substantially contributes to the LCOD: with free waste heat the cost could be further reduced to 278 € $t_{CO2}^{-1}$. If the $CO_2$ level is increased by controlling the ventilation to hold a certain concentration in the indoor air, the energy demand is lower than with an uncontrolled system, but the lower capture capacity will lead to a substantial increase in capture costs, resulting in numbers closer to 800 € t $t_{CO2}^{-1}$. Even if the adsorber is designed smaller for that case, the even lower capture rate will increase the LCOD. In summary, it can be said that DAC systems benefit from the most affordable energy sources and densely populated buildings, ideally with several units sharing desorption equipment.

In summary, it can be said that we consider the concept of decentralized DAC plants, embedded in the Crowd Oil concept, to be economically viable and that research into this approach should be continued accordingly. Practical problems such as the transport of the captured $CO_2$, whether by truck or repurposed gas networks, as well as its reuse or permanent disposal, should be addressed in the future. Only in this way can a sufficiently rapid ramp-up take place to effectively support climate targets.

## CRediT authorship contribution statement

**Dominik Heß:** Writing – original draft, Visualization, Software, Methodology, Investigation, Formal analysis. **Michael Rubin:** Writing – review & editing, Project administration. **Roland Dittmeyer:** Writing – review & editing, Supervision, Funding acquisition.

## Declaration of Competing Interest

The authors declare that they have no known competing financial interests or personal relationships that could have appeared to influence

the work reported in this paper.

## Acknowledgements

This work was performed as part of the projects 'Helmholtz-Climate-Initiative' (HI-CAM) and 'A Comprehensive Approach to Harnessing the Innovation Potential of Direct Air Capture and Storage for Reaching $CO_2$-Neutrality' (DACStorE, Grant Agreement Number KA2-HSC-12), which are funded by the Initiative and Networking Fund of the Helmholtz Association.

## Appendix A. Supporting information

Supplementary data associated with this article can be found in the online version at doi:10.1016/j.jcou.2026.103351.

## Data Availability

Data will be made available on request.

## References

[1] UNFCCC, The Paris Agreement. [Online]. Available: ⟨https://unfccc.int/process-and-meetings/the-paris-agreement/the-paris-agreement⟩.
[2] P. Friedlingstein, et al., Global Carbon Budget 2024, Earth Syst. Sci. Data 17 (3) (2025) 965–1039, https://doi.org/10.5194/essd-17-965-2025.
[3] Roadmap Chemie 2050 auf dem Weg zu einer treibhausgasneutralen chemischen Industrie in Deutschland: eine Studie von DECHEMA und FutureCamp für den VCI. Frankfurt am Main: DECHEMA Gesellschaft für Chemische Technik und Biotechnologie e.V, 2019.
[4] P. Viebahn, A. Scholz, O. Zelt, The potential role of direct air capture in the german energy research program—results of a multi-dimensional analysis, Energies 12 (18) (2019) 3443, https://doi.org/10.3390/en12183443.
[5] M. Bui, Di Zhang, M. Fajardy, N. Mac Dowell, Delivering carbon negative electricity, heat and hydrogen with BECCS – Comparing the options, Int. J. Hydrog. Energy 46 (29) (2021) 15298–15321, https://doi.org/10.1016/j.ijhydene.2021.02.042.
[6] M. Fajardy, J. Morris, A. Gurgel, H. Herzog, N. Mac Dowell, S. Paltsev, The economics of bioenergy with carbon capture and storage (BECCS) deployment in a 1.5 °C or 2 °C world, Glob. Environ. Change 68 (2021) 102262, https://doi.org/10.1016/j.gloenvcha.2021.102262.
[7] H. Li, Y. Tan, M. Ditaranto, J. Yan, Z. Yu, Capturing CO2 from biogas plants, Energy Procedia (114) (2017) 6030–6035, https://doi.org/10.1016/j.egypro.2017.03.1738.
[8] H. Bouaboula, J. Chaouki, Y. Belmabkhout, A. Zaabout, Comparative review of direct air capture technologies: from technical, commercial, economic, and environmental aspects, Chem. Eng. J. 484 (2024) 149411, https://doi.org/10.1016/j.cej.2024.149411.
[9] E.S. Sanz-Pérez, C.R. Murdock, S.A. Didas, C.W. Jones, Direct capture of CO2 from ambient air, Chem. Rev. (116) (2016) 11840–11876, https://doi.org/10.1021/acs.chemrev.6b00173.
[10] M. Ozkan, S.P. Nayak, A.D. Ruiz, W. Jiang, Current status and pillars of direct air capture technologies, iScience 25 (4) (2022) 103990, https://doi.org/10.1016/j.isci.2022.103990.
[11] M.D. Eisamann, et al., Energy-efficient electrochemical CO2 capture from the atmosphere, TechConnect Briefs Tech. Proc. 2009 Clean. Technol. Conf. Trade Show. (2009) 175–178.
[12] S. Voskian, T.A. Hatton, Faradaic electro-swing reactive adsorption for CO2 capture, Energy Environ. Sci. 12 (12) (2019) 3530–3547, https://doi.org/10.1039/C9EE02412C.
[13] D.W. Keith, G. Holmes, D. St. Angelo, K. Heidel, A process for capturing CO2 from the atmosphere, Joule (2) (2018) 1573–1594, https://doi.org/10.1016/j.joule.2018.05.006.
[14] Carbon Engineering, Oxy Low Carbon Ventures, Rusheen Capital Management create development company 1PointFive to deploy Carbon Engineering's Direct Air Capture technology. [Online]. Available: ⟨https://carbonengineering.com/news-updates/new-development-company-1pointfive-formed/⟩.
[15] J.A. Wurzbacher, C. Gebald, N. Piatkowski, A. Steinfeld, Concurrent separation of CO2 and H2O from air by a temperature-vacuum swing adsorption/desorption cycle, Environ. Sci. Technol. (46) (2012) 9191–9198, https://doi.org/10.1021/es301953k.
[16] C. Gebald, J.A. Wurzbacher, P. Tingaut, T. Zimmermann, A. Steinfeld, Amine-based nanofibrillated cellulose as adsorbent for CO\textsubscript{2} capture from air, Environ. Sci. Technol. (45) (2011) 9101–9108, https://doi.org/10.1021/es202223p.
[17] J. Young, E. García-Díez, S. Garcia, M. Van Der Spek, The impact of binary water–CO $_2$ isotherm models on the optimal performance of sorbent-based direct air capture processes, Energy Environ. Sci. 14 (10) (2021) 5377–5394, https://doi.org/10.1039/D1EE01272J.
[18] X. Zhu, et al., Recent advances in direct air capture by adsorption, Chem. Soc. Rev. 51 (15) (2022) 6574–6651, https://doi.org/10.1039/D1CS00970B.
[19] A. Sodiq, et al., A review on progress made in direct air capture of CO 2, Environ. Technol. Innov. 29 (2023) 102991, https://doi.org/10.1016/j.eti.2022.102991.
[20] Mammoth: Our Newest Facility, 2022. Accessed: Nov. 19, 2024. [Online]. Available: ⟨https://climeworks.com/plant-mammoth⟩.
[21] Soletair Power Carbon Capture Technology. Accessed: Feb. 14, 2024. [Online]. Available: ⟨https://www.soletairpower.fi/technology/⟩.
[22] Skytree Website. Accessed: Feb. 14, 2024. [Online]. Available: ⟨https://www.skytree.eu/⟩.
[23] L. Baus, S. Nehr, Potentials and limitations of direct air capturing in the built environment, Build. Environ. 208 (2022) 108629, https://doi.org/10.1016/j.buildenv.2021.108629.
[24] J.P. Harrouz, K. Ghali, M. Hmade, and N. Ghaddar, Carbon capture from indoor air as an alternative ventilation technique, presented at the REHVA 14th HVAC World Congress, Rotterdam: Clima2022, 2022.
[25] M.K. Kim, L. Baldini, H. Leibundgut, J.A. Wurzbacher, N. Piatkowski, A novel ventilation strategy with CO2 capture device and energy saving in buildings, Energy Build. 87 (2015) 134–141, https://doi.org/10.1016/j.enbuild.2014.11.017.
[26] Y. Xu, X. Han, X.E. Cao, Comprehensive performance evaluation of HVAC systems integrated with direct air capture of CO2 in various climate zones, Build. Environ. 266 (2024) 112048, https://doi.org/10.1016/j.buildenv.2024.112048.
[27] R. Dittmeyer, M. Klumpp, P. Kant, G. Ozin, Crowd oil not crude oil, Nat. Commun. 10 (1) (2019) 1818, https://doi.org/10.1038/s41467-019-09685-x.
[28] O.A. Seppanen, W.J. Fisk, M.J. Mendell, Association of ventilation rates and CO2 concentrations with health and other responses in commercial and institutional buildings, Indoor Air 9 (4) (1999) 226–252, https://doi.org/10.1111/j.1600-0668.1999.00003.x.
[29] W. Cheng, et al., Global monthly gridded atmospheric carbon dioxide concentrations under the historical and future scenarios, Sci. Data 9 (1) (2022) 83, https://doi.org/10.1038/s41597-022-01196-7.
[30] J. Wilcox, Carbon Capture, Springer Science+Business Media, New York, Dordrecht, Heidelberg, London, 2012.
[31] F. Sabatino, A. Grimm, F. Gallucci, M. Van Sint Annaland, G.J. Kramer, M. Gazzani, A comparative energy and costs assessment and optimization for direct air capture technologies, Joule 5 (8) (2021) 2047–2076, https://doi.org/10.1016/j.joule.2021.05.023.
[32] D. Heß, M. Klumpp, R. Dittmeyer, and Verkehrsmininsterium Baden-Württemberg, Nutzung von CO2 aus Luft als Rohstoff für synthetische Kraftstoffe und Chemikalien,. 2020. [Online]. Available: ⟨https://vm.baden-wuerttemberg.de/fileadmin/redaktion/m-mvi/intern/Dateien/PDF/29-01-2021-DAC-Studie.pdf⟩.
[33] M. Fasihi, O. Efimova, C. Breyer, Techno-economic assessment of CO2 direct air capture plants, J. Clean. Prod. (224) (2019) 957–980, https://doi.org/10.1016/j.jclepro.2019.03.086.
[34] Bundesanstalt für Arbeitsschutz und Arbeitsmedizin (BAuA), ASR A1.2 Raumabmessungen und Bewegungsflächen. 2022.
[35] J.A. Wurzbacher, C. Gebald, S. Brunner, A. Steinfeld, Heat and mass transfer of temperature–vacuum swing desorption for CO2 capture from air, Chem. Eng. J. 283 (2016) 1329–1338, https://doi.org/10.1016/j.cej.2015.08.035.
[36] J. Young, E. García-Díez, S. Garcia, C. Ireland, B. Smit, M. Van Der Spek, Investigating H2O and CO2 co-adsorption on amine-functionalised solid sorbents for direct air capture, SSRN Electron. J. (2021), https://doi.org/10.2139/ssrn.3814942.
[37] PRODUCT INFORMATION LEWATIT® VP OC 1065, Lanxess AG, 2024. Accessed: Feb. 10, 2025. [Online]. Available: ⟨https://lanxess.com/en-us/products-and-brands/products/l/lewatit–vp-oc-1065⟩.
[38] Gesundheitliche Bewertung von Kohlendioxid in der Innenraumluft: Mitteilungen der Ad-hoc-Arbeitsgruppe Innenraumrichtwerte der Innenraumlufthygiene-Kommission des Umweltbundesamtes und der Obersten Landesgesundheitsbehörden, Bundesgesundheitsblatt - Gesundheitsforschung - Gesundheitsschutz, vol. 51, no. 11, pp. 1358–1369, Nov. 2008, doi: 10.1007/s00103-008-0707-2.
[39] A. Persily, L. Jonge, Carbon dioxide generation rates for building occupants, Indoor Air 27 (5) (2017) 868–879, https://doi.org/10.1111/ina.12383.
[40] R. Urbaniak, B. Ciupek, P. Grobelny, Experimental analysis of vacuum solar collectors as an auxiliary heating source for residential buildings, Energies 18 (5) (2025) 1093, https://doi.org/10.3390/en18051093.
[41] O.O. Soneye, M.A. Ayoola, I.A. Ajao, O.O. Jegede, Diurnal and seasonal variations of the incoming solar radiation flux at a tropical station, Ile-Ife, Nigeria, Heliyon 5 (5) (2019) 01673, https://doi.org/10.1016/j.heliyon.2019.e01673.
[42] VDI-Wärmeatlas, 11., Bearb. und erw. Aufl. in Springer eBook Collection. Berlin, Heidelberg: Springer Vieweg, 2013. doi: 10.1007/978-3-642-19981-3.
[43] D.D. Do, Adsorption analysis: equilibria and kinetics (no), in: Series on chemical engineering, v 2, Imperial College Press, London, 1998.
[44] F.J. Gutiérrez Ortiz, M. Barragán Rodríguez, R.T. Yang, Modeling of fixed-bed columns for gas physical adsorption, Chem. Eng. J. 378 (2019) 121985, https://doi.org/10.1016/j.cej.2019.121985.
[45] M.F. Edwards, J.F. Richardson, Gas dispersion in packed beds, Chem. Eng. Sci. 23 (2) (1968) 109–123, https://doi.org/10.1016/0009-2509(68)87056-3.
[46] P. Edinger, D. Grimekis, K. Panopoulos, S. Karellas, C. Ludwig, Adsorption of thiophene by activated carbon: a global sensitivity analysis, J. Environ. Chem. Eng. 5 (4) (2017) 4173–4184, https://doi.org/10.1016/j.jece.2017.07.041.
[47] R. Krishna, J.M. Van Baten, Investigating the validity of the Bosanquet formula for estimation of diffusivities in mesopores, Chem. Eng. Sci. 69 (1) (2012) 684–688, https://doi.org/10.1016/j.ces.2011.11.026.

[48] E. dward, N. Fuller, K. Ensley, J.C. Giddings, Diffusion of halogenated hydrocarbons in helium: the effect of structure on collision cross sections, J. Phys. Chem. 78 (11) (1968).
[49] U. Caldera, D. Bogdanov, C. Breyer, Local cost of seawater RO desalination based on solar PV and wind energy: a global estimate, Desalination 385 (2016) 207–216, https://doi.org/10.1016/j.desal.2016.02.004.
[50] U. Caldera, C. Breyer, Learning curve for seawater reverse osmosis desalination plants: capital cost trend of the past, present, and future, Water Resour. Res. 53 (12) (2017) 10523–10538, https://doi.org/10.1002/2017WR021402.
[51] H.G. Hirschberg, Handbuch Verfahrenstechnik und Anlagenbau: Chemie, Technik, Wirtschaftlichkeit; mit 689 Tabellen, Springer, Berlin Heidelberg, 1999.
[52] F. Sabatino, et al., Evaluation of a direct air capture process combining wet scrubbing and bipolar membrane electrodialysis, Ind. Eng. Chem. Res. 59 (15) (2020) 7007–7020, https://doi.org/10.1021/acs.iecr.9b05641.
[53] A. Lee, D.C. Miller, A one-dimensional (1-D) three-region model for a bubbling fluidized-bed adsorber, p. 121219160808001, Ind. Eng. Chem. Res. (2012), https://doi.org/10.1021/ie300840q.
[54] R.S. Maier, D.M. Kroll, H.T. Davis, Diameter-dependent dispersion in packed cylinders, AIChE J. 53 (2) (2007) 527–530, https://doi.org/10.1002/aic.11083.
[55] J.M.P.Q. Delgado, A critical review of dispersion in packed beds, Heat. Mass Transf. 42 (4) (2006) 279–310, https://doi.org/10.1007/s00231-005-0019-0.
[56] M. Papapetrou, G. Kosmadakis, A. Cipollina, U. La Commare, G. Micale, Industrial waste heat: estimation of the technically available resource in the EU per industrial sector, temperature level and country, Appl. Therm. Eng. 138 (2018) 207–216, https://doi.org/10.1016/j.applthermaleng.2018.04.043.
[57] A.G. Malanichev, P.V. Vorobyev, Forecast of global steel prices, Stud. Russ. Econ. Dev. 22 (3) (2011) 304–311, https://doi.org/10.1134/S1075700711030105.
[58] Agora Energiewende,'Studie: Current and Future Cost of Photovoltaics: Long-term Scenarios for Market Development, System Prices and LCOE of Utility-Scale PV Systems, Jan. 2015. [Online]. Available: ⟨https://www.ise.fraunhofer.de/content/dam/ise/de/documents/publications/studies/AgoraEnergiewende_Current_and_Future_Cost_of_PV_Feb2015_web.pdf⟩.
[59] K. Sievert, T.S. Schmidt, B. Steffen, Considering technology characteristics to project future costs of direct air capture, p. S2542435124000606, Joule (2024), https://doi.org/10.1016/j.joule.2024.02.005.
[60] T. Roestenberg and ANTECY, Design Study Report: ANTECY solar fuels development, Hoelaken, the Neatherlands, 2015. [Online]. Available: ⟨https://www.antecy.com/Images/Design%20study%20report%20FINAL.pdf⟩.
[61] K.S. Lackner, H. Azarabadi, Buying down the cost of direct air capture, Ind. Eng. Chem. Res. 60 (22) (2021) 8196–8208, https://doi.org/10.1021/acs.iecr.0c04839.

## Glossary

### Nomenclature

*AC:* Air Conditioning
*BECCS:* Bioenergy with CCS
*CAPEX:* Capital Expenditures
*CCU:* Carbon Capture and Utilization
*CCS:* Carbon Capture and Storage
*CDR:* Carbon Dioxide Removal
*$CO_2$:* Carbon Dioxide
*COP:* Coefficient of Performance
*COP21:* 21st Conference of the Parties
*CSTR:* Continuously Stirred Tank Reactor
*DAC:* Direct Air Capture
*EPA:* Environmental Protection Agency
*GAB:* Guggenheim, Anderson, Boer
*GHG:* Green House Gas
*$Gt_C$:* Gigaton Carbon
*$GT_{CO2}$:* Gigaton $CO_2$
*HT-DAC:* High Temperature- DAC
*HVAC:* Heating, Ventilation and Air Conditioning
*IMVT:* Institute for Micro Process Engineering
*IPCC:* Intergovernmental Panel on Climate Change
*LCOD:* Levelized Cost of DAC
*LT-DAC:* Low Temperature- DAC
*LW:* Lewatit
*MOF:* Metal Organic Framework
*Mt:* Megaton
*NC:* Nanocellulose
*OB:* Office Building
*OPEX:* Operational Expenditures
*OPO:* Open Plan Office
*PFR:* Plug Flow Reactor
*SP:* Setpoint
*TRL:* Technology Readiness Level
*TPSA:* Temperature Pressure Swing Adsorption
*TVSA:* Temperature Vacuum Swing Adsorption
*UBA:* Umweltbundesamt
*WADST:* Weighted Average Dual Site Toth-Model
*WH:* Warehouse

### Symbols

*A:* Area ($m^2$), Coefficient Isotherm (-)
*$\beta$:* Mass transfer coefficient ($m\ s^{-1}$)
*b:* Coefficient Isotherm (-)
*c:* Concentration ($mol\ m^{-3}$)
*C:* Coefficient Isotherm (-)
*D:* Diffusion/ Dispersion coefficient ($m^2\ s^{-1}$)
*d:* Diameter (m)
*$D_{ax}$:* Axial Dispersion Coefficient ($m^2\ s^{-1}$)
*$\varepsilon$:* Porosity (-)
*$\eta$:* Efficiency (-), Dynamic Viscosity (Pa s)
*$f_{RH}$:* Enhancement Factor
*$\dot{G}$:* Total $CO_2$ generation rate ($L_{CO2}\ s^{-1}$)
*$\dot{g}$:* Per person $CO_2$ generation rate ($L_{CO2}\ s^{-1}\ Person^{-1}$)
*k:* Heat Conductivity ($W\ m^{-1}\ K^{-1}$), Kinetic Coefficient ($s^{-1}$)
*$\kappa$:* Isentropic Exponent (-)
*L:* Length (m)
*LR:* Learning Rate (%)
*$\dot{m}$:* Mass Flow (kg s-1)
*M:* Molar Mass ($kg\ mol^{-1}$)
*n:* Number (-), Coefficient (n)
*p:* (Partial) Pressure (Pa)
*$\Delta p$:* Pressure Drop (Pa)
*P:* Power (W)
*Pe:* Peclet Number (-)
*$\phi$:* Relative Humidity (-)
*PR:* Production Rate (%)
*q:* Loading ($mol\ kg^{-1}$)
*R:* Universal Gas Constant ($J\ mol^{-1}\ K^{-1}$)
*Re:* Reynolds Number (-)
*$\rho$:* Density ($kg\ m^{-3}$)
*Sc:* Schmidt Number (-)
*Sh:* Sherwood Number (-)
*t:* time (s, min, h)
*T:* Temperature (K, °C)
*u:* velocity ($m\ s^{-1}$)
*$\tau$:* Tortuosity (-), Coefficient Isotherm (-)
*$\nu$:* Kinematic Viscosity ($m\ s^{-2}$), Effective Molecular Volume ($m^3$)
*V:* Volume ($m^3$)
*$\dot{V}$:* Volume Flow ($m^3$ s-1)
*z:* Length variable (m)

### Index

*0:* Initial
**:* Equilibrium
*air:* Air
*add:* Additional
*ads:* Adsorption
*ax:* Axial
*Base:* Base (lowest)
*bed:* Adsorber Bed
*buil:* Building
*cap:* Capture
*chamber:* In the Chamber
*CO2:* Carbon Dioxide
*DAC:* Direct Air Capture
*dry:* dry conditions
*eff:* Effective
*el:* Electric
*f:* Fluid
*fix:* Fixed
*Fan:* Fan
*G, gas:* Gas
*H2O:* Water
*I:* Index
*in:* Intake
*Knudsen:* Knudsen Diffusion
*LDF:* Linear Driving Force
*m:* Molecular
*max:* Maximum
*nom:* Nominal
*out:* Exhaust
*Part:* Particle
*People:* People
*Pore:* Pore
*S:* Solid
*th:* Thermal
*tot:* total
*Vac:* Vaccum (pump)
*var:* Variable
*wet:* Wet conditions